

**CYCLONE TESTING STATION**

**FATIGUE BEHAVIOUR OF CORRUGATED ROOFING**

**UNDER CYCLIC WIND LOADING**

**by**

**M. MAHENDRAN**

**TECHNICAL REPORT No. 35**

**MAY 1989**

© James Cook Cyclone Structural Testing Station

Mahendran, Mahadeva, 1956-

Fatigue behaviour of corrugated roofing under cyclic  
wind loading.

ISBN 0 86443 314 X.

ISSN 0158 - 8338

1. Sheet-metal, Corrugated - Testing. 2. Roofing, Iron  
and steel - Testing. 3. Wind-pressure. I. James Cook  
University of North Queensland. Cyclone Testing Station.  
II. Title. (Series : Technical report (James Cook  
University of North Queensland. Cyclone Testing  
Station) ; no. 35).

690'.15

## TABLE OF CONTENTS

	Page
NOTATION	
ABSTRACT	
1. INTRODUCTION	1
1.1 Background	
1.2 Present Problem	
1.3 Objectives and Method of Investigation	
2. LITERATURE REVIEW	3
2.1 General	
2.2 Metal Fatigue	
2.3 Wind Induced Fatigue of Metal Roof Claddings	
2.4 Fatigue Investigations on Corrugated Roof Claddings	
2.5 Simulation of Wind Fatigue Loading	
3. EXPERIMENTAL METHOD	8
3.1 General	
3.2 Simulation of Wind Loading	
3.3 Test Specimen	
3.4 Test Set-up	
3.5 Types of Tests	
3.6 Testing Method	
4. RESULTS AND DISCUSSION	16
4.1 General	
4.2 Roofing Fastened at Alternate Crests without Cyclone Washers	17
4.2.1 Cycling from zero minimum load	
4.2.2 Cycling from nonzero minimum load	
4.2.3 General equation to predict $N_f$ for all loading cases	
4.2.4 Effect of initially tightened fasteners	
4.2.5 Effect of loading frequency	
4.3 Roofing Fastened at Alternate Crests with Cyclone Washers	36
4.4 Roofing Fastened at Every Crest without Cyclone Washers	41
4.5 Roofing Fastened at Alternate Valleys	43

5. IMPLICATIONS OF THE RESULTS OBTAINED	46
5.1 Comparison of Fatigue Performance of Roofing with Different Fastening Systems	
5.2 Current Design Loads in Relation to LPD Load	
5.2.1 Alternate crest fastening without cyclone washers	
5.2.2 Alternate crest fastening with cyclone washers	
5.3 Current Situation Regarding Safety of Roofing Subjected to Cyclonic Wind Loading	
5.4 Other Roofing Profiles	
5.5 Future Work	
5.6 Other Comments	
6. CONCLUSIONS AND RECOMMENDATIONS	54
7. ACKNOWLEDGEMENTS	58
8. REFERENCES	58

## NOTATION

1.	D	-	Accumulated Fatigue Damage in Eqn. 1
2.	DL	-	Working Design Load
3.	L	-	Span in Eqn.2
4.	LPD	-	Local Plastic Buckling Deformation
5.	M	-	Bending Moment at the Central Support in Eqn.2
6.	N/f	-	Newtons per Fastener
7.	N <sub>f</sub>	-	Number of Cycles to Fatigue Failure
8.	N <sub>i</sub>	-	Number of Cycles to Crack Initiation
9.	N <sub>j</sub>	-	Number of Cycles required to Cause Fatigue Failure at Load Level S <sub>j</sub> in Eqn.1
10.	n <sub>j</sub>	-	Number of Cycles Applied at Load Level S <sub>j</sub> in Eqn.1
11.	P	-	Average Load per Fastener at the Central Support in Eqn.2
12.	P <sub>b</sub>	-	Local Plastic Buckling Load per Fastener
13.	P <sub>max</sub>	-	Average Maximum Cyclic Load per Fastener
14.	P <sub>u</sub>	-	Ultimate Design Wind Load per Fastener
15.	R	-	Range of Cyclic Loading per Fastener



## ABSTRACT

Low cycle fatigue cracking of light gauge metal roofing was investigated by testing a number of two-span corrugated roofing assemblies under cyclic uplift wind loading. A large number of constant amplitude fatigue tests from zero or nonzero minimum load to various maximum loads was conducted for different spans and fastening systems.

The results revealed the dependence of fatigue behaviour of corrugated roofing on the type of fastening system used. Fatigue test results correlated well with the corresponding static results reported earlier. Many types of cracks were observed depending on the type of fastening system used and the cyclic load levels. A comparison was made of the superiority of one fastening system over the other regarding fatigue performance.

When the most common fastening system in cyclonic areas, the alternate crest fastening without cyclone washers was used during tests with zero minimum load, the fatigue curves had different segments because of the premature local plastic buckling deformation (LPD) at approximately 550 to 650 N per fastener around the fastener holes. Large stress concentrations in this region caused low cycle fatigue cracking for all the spans of roofing. When the maximum cyclic load exceeded the LPD load, the fatigue performance deteriorated rapidly as the same region yielded at the LPD load. Despite the presence of reserve static strength the LPD load should be considered the ultimate fatigue load. Some anomalous results were obtained due to the presence of this local plastic buckling behaviour. It was found that not only maximum cyclic load was critical, but also range of loading. Tests on different spans showed that load per fastener was the most critical fatigue parameter in this case whereas both load per fastener and bending moment at the central support were critical for all other fastening systems.

When alternate crests were fastened with cyclone washers, the fatigue performance was improved significantly as the region around the fastener holes was free of large stress concentrations due to greater local plastic buckling load. Alternate valley fastening or every crest fastening also improved the fatigue performance as no local plastic buckling behaviour existed in these cases. However, only alternate crest fastening with cyclone washers was recommended due to some shortcomings inherent with the other two fastening systems.

Fatigue characteristics in the form of a matrix of cycles to fatigue failure for various combinations of range and mean level of loading was developed for corrugated roof claddings fastened at alternate crests without cyclone washers. This is being used in the analysis and testing to review the current standard fatigue tests.

## 1. INTRODUCTION

### 1.1 Background

On Christmas day 1974, the northern Australian city of Darwin was devastated by cyclone Tracy. Wind damage investigations following cyclone Tracy revealed the extensive damage to light gauge metal roof claddings which are the dominant form of roofing in the tropical cyclone prone areas of Australia. This premature failure of roofing led to the failure of other structural elements due to overloading and/or instability, and to the collapse of the entire house eventually. Failure of some houses caused the other houses to be exposed to high winds and flying debris attack and thus the failure spread like a chain reaction (Walker, 1975). In fact, the overall damage to housing caused by cyclone Tracy was extensive, for example, 50 to 60% of traditional timber houses were damaged beyond repair, and over 90% of houses and 70% of all other structures suffered considerable damage to roofing (Walker, 1975). It was considered that cyclone Tracy was the most disastrous single event to have occurred in Australian history in terms of its impact on the community (Walker, 1980). Morgan and Beck (1977) and Beck and Morgan (1975) carried out laboratory and field investigations to determine the cause of this roofing failure and concluded that the main reason for such a widespread damage to roofing during cyclone Tracy was the fatigue failure in the vicinity of its fasteners.

Following cyclone Tracy, drastic steps were taken by such requirements that all small buildings including housing are to be structurally engineered and all roofing assemblies are to be fatigue tested according to Darwin Area Building Manual (DABM) (DRC, 1976) and TR440 (EBS, 1978). The DABM test (described in Section 2.5) was introduced soon after cyclone Tracy on which the reconstruction of Darwin was based, and is still being used in the Northern Territory (N.T.). The TR440 test (described in Section 2.5) which is considered to simulate more closely the random nature of wind loading on roof claddings was introduced later based on studies by Melbourne (1977) and Beck (1977). The latter test is widely used in all the cyclone prone areas of Australia, except in N.T. A large cyclone washer capable of preventing premature fatigue failure was developed as the immediate solution to the fatigue failure at the fastener holes. These and other significant changes to the Australian building regulations and practice have been presented by Walker (1980). Further fatigue investigation was carried out by Beck and Stevens (1979) on corrugated roof claddings to improve the knowledge on the behaviour of light gauge metal roofing under cyclic uplift wind loading.

All these steps to improve the fatigue performance of light gauge metal roofing did in fact improve the fatigue performance as evident during recent cyclones (Reardon et al., 1986). However, it is still considered that light gauge metal roofing assemblies may be vulnerable in cyclonic winds.

## 1.2 Present Problem

The standard fatigue tests described in TR440 and DABM, the results of which could depend on so many sensitive parameters such as the initial tightening of fasteners, are only providing an approximate answer to the complicated low cycle fatigue problem under rapidly fluctuating cyclonic winds. There have been reports of instances when the roofing systems which passed these tests did not appear to be very much different to those which failed during cyclone Tracy. Such anomalies arising from testing indicate the possibility of these fatigue tests being inadequate for their intended purpose. The fact that two different fatigue tests are being used to assess the fatigue strength of the roofing assemblies within the same cyclonic region of Australia reflects the doubts that prevail regarding these tests. It is considered that the research base for these fatigue tests is relatively small compared with that on which most structural engineering criteria are based (Walker and Reardon, 1986).

A major wind tunnel study has been completed recently at James Cook University which provided a comprehensive data base on the fatigue characteristics of wind pressure on roof claddings. This data base is now to be used to simulate the fatigue damage resulting from the passage of tropical cyclones that will enable a review of current fatigue testing methods. For this to be achieved a comprehensive data base on the fatigue failure characteristics of the typical light gauge metal roof claddings is required by means of extensive laboratory testing of such claddings.

Further it is to be noted that the section properties of light gauge metal roofing profiles and the strength properties of sheet material have changed significantly towards high strength and thinner roofing in recent times. Although light gauge metal roofing profiles have been in use for a long time, their use has been mainly based on some limited static and fatigue test results.

At the time when the cyclone washer-fastener assemblies were developed, it was believed that the fatigue problem of light gauge metal roofing has been rectified. This cannot be true as these washers which are unpopular among the builders are not commonly used except in the N.T. It is further noted that these washers have become thinner following the same trend as roofing. Therefore in another cyclone of similar or greater magnitude than Tracy, the light gauge metal roofing assemblies may still be susceptible to fatigue damage.

Hence the Cyclone Testing Station is currently conducting a detailed investigation into the behaviour of light gauge metal roofing with emphasis on corrugated roofing. Although a wide range of profiled roof claddings is currently available in Australia, corrugated roofing was chosen for this investigation as it is reportedly the most common roofing profile in the cyclone prone areas of Australia.

### **1.3 Objectives and Method of Investigation**

This investigation has two broad objectives. The first is to gain a much better basic understanding of the fatigue phenomenon by identifying the structural and material parameters which cause fatigue cracking and to develop design recommendations towards eliminating fatigue failures. The second is to look at the other aspect of developing a new standard fatigue testing method for the whole of Australian cyclone prone areas if current ones are found to be inadequate. The first objective involves a static investigation of corrugated roofing fastened with different fastening systems and spans, a study of the effects of relevant loading parameters on fatigue behaviour, observing various types of fatigue cracks and obtaining details on crack initiation and propagation, obtaining the so-called S-N fatigue curves and correlating results from static and fatigue investigations. The investigation described in this report attempts to achieve fully the first objective, and partly the second objective by developing the database of fatigue characteristics of corrugated roof claddings.

In this investigation it was decided to study the fatigue behaviour of roof claddings under uplift wind loading alone. Wind damage investigations after cyclone Tracy indicated that fatigue failure of roofing was due to fluctuating uplift loading only and not due to in-plane shear loads (Beck and Morgan, 1975). However, it is now believed that roof claddings carry part of lateral loading due to wind, and another investigation is currently under way that includes the effects of combined uplift and in-plane shear forces on fatigue cracking.

Analytical and experimental studies of corrugated roofing assemblies with different spans and fastening systems were first conducted under static uplift wind loading conditions as part of this investigation and their results have been already reported in Mahendran (1988b). The same roofing assemblies were then subjected to cyclic uplift wind loading. This report presents the results of these fatigue tests in detail.

## **2. LITERATURE REVIEW**

### **2.1 General**

In this fatigue investigation on light gauge steel roof claddings, cracks initiated in a small area around the fastener holes and propagated till the fasteners could pull through the roofing. Therefore research work on metal fatigue involving initiation and propagation of cracks is relevant to this investigation. Research work on metal fatigue has been very extensive since the time when metal fatigue failure was first observed in the middle of 19th century. Most of this work has been mainly addressing problems related to the aircraft industry. In general all metal fatigue research work may involve one or more of the following topics.

- Structural investigation involving general stress analysis, stress concentrations, identification of parameters causing fatigue cracking, etc.
- Fracture mechanics approach to predict fatigue failure
- Metallurgical study
- Simulation of realistic fatigue loading on the structure
- Estimation of accumulated fatigue damage due to variable amplitude loadings

Although this investigation at this stage falls mainly into the first group above, a brief review of metal fatigue related to other groups is also presented in this section.

During the last decade particularly after cyclone Tracy, a number of fatigue investigations were carried out on corrugated roof claddings. Brief details of these investigations are also presented in this section.

## 2.2 Metal Fatigue

Fatigue is a progressive process through many phases such as cyclic slip, crack nucleation, growth of microcracks, growth of macrocracks and final failure. In the absence of cracks or crack-like defects prior to loading, crack initiation occurs at points of stress concentration on the surface. The tragedy of the fatigue resistance of metals is that even when the surface is highly polished and no stress concentrations are present, cracks can initiate if the cyclic stress amplitude and number of cycles of applied loading are large enough. The key to crack initiation is cyclic plastic strain that is present in a few isolated surface grains or in well-defined plastic zones.

Cyclic slip occurs at the plane of least slip resistance which is parallel to a maximum shear stress plane and this starts the fatigue process. This shear mode propagation is soon replaced by a tensile mode propagation. When the crack has developed sufficiently the failure will occur as the remaining uncracked section of the member can no longer resist the applied load.

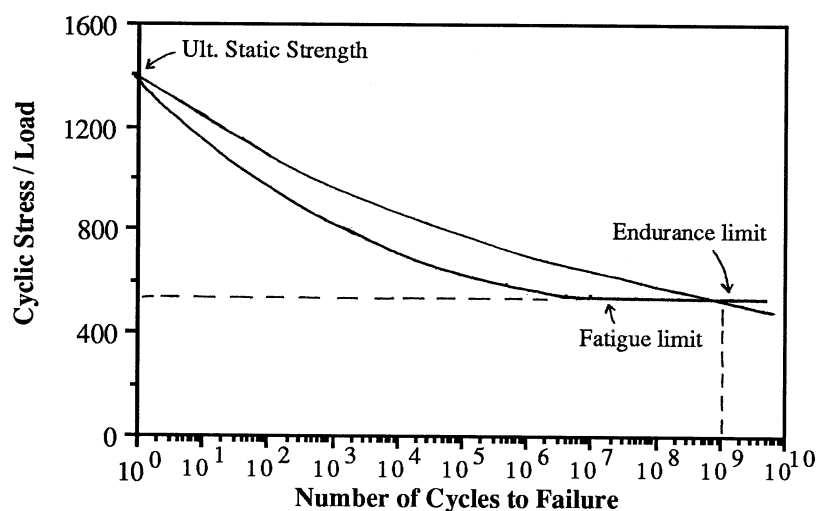


Figure 1. Typical S-N Curve

It has been traditional to use the so-called S-N curves (see Figure 1) of cyclic stress/load versus fatigue life (number of cycles to failure  $N_f$ ) derived from constant amplitude load tests for fatigue design purposes. The S-N curves are plotted with the horizontal axis of fatigue life on a  $\log_{10}$  scale and the vertical axis of stress/load on a linear scale, but very often the latter is also plotted on a  $\log_{10}$  scale in order to obtain a mathematical relationship between the two variables. The significant features of this curve are that as the fluctuating stress level is decreased the fatigue life increases and eventually a fatigue limit or an endurance limit is reached. A fatigue limit is the stress level below which no fatigue failure will occur irrespective of the number of cycles of loading applied whereas an endurance limit is the stress level for a very high  $N_f$  (usually  $10^9$ ) which is considered the upper limit of the number of cycles of loading the member will be subjected to during its intended life span. Usually the ratio of fatigue limit or endurance limit to ultimate static strength is between 0.4 and 0.5 for most steels. This ratio is very much dependent on a number of variables such as stress concentrations due to notches, residual tension or compression, surface irregularities and other defects.

Originally the S-N curves were developed for loadings with a zero mean stress. In order to account for other values of mean stress, many empirical laws such as Gerber's law, modified Goodman's law and Soderberg's law were developed (D'Isa, 1968). These laws include the effect of notch sensitivity as well.

The use of a traditional approach based on S-N curves leads to difficulties because it does not give any information on the relative contribution of crack initiation and crack propagation to total fatigue life. In most cases virtually the whole fatigue life is occupied by fatigue crack growth. Therefore the testing and design need to be based on fatigue crack growth properties. The fracture mechanics approach has been extensively used for this purpose. Linear elastic fracture mechanics principles using the concept of stress intensity factors or elastic-plastic fracture mechanics principles are used depending on the presence or absence of plasticity at the cracked zones (elastic or plastic fracture). Prediction of fatigue failure can be achieved by using the appropriate laws in this approach. Details of such applications are given in many excellent books such as Atkins and Mai (1985), Rolfe and Barsom (1977) and Owen and Fawkes (1983).

Apart from the above work on fatigue, metallurgical study forms another important branch from which a vast amount of fatigue information has been gained in the past. This study essentially involved determination of various microscopic mechanisms responsible for initiation of fatigue cracks and the role of microstructure, that is, how the observed fatigue failures were related to microstructure. This study at microscopic level has been used in the past to develop new materials and design details with improved fatigue resistance.

In reality the loading on aircraft during service or on roof claddings due to cyclonic winds is of a variable amplitude type. This requires realistic simulation of loading and the use of a valid law to

estimate the fatigue damage for a safe design. In this respect, there has been a number of investigations on aircraft and off-shore structures (Ekvall and Young, 1976, Pook, 1978). Although a wide variety of cumulative damage theories has been developed, the most commonly used one is Miner's law which is a simple linear cumulative fatigue theory. According to Miner's law, the fatigue damage accumulated 'D' due to loadings of more than one amplitude (k) is given by

$$D = \sum_{j=1}^k \frac{n_j}{N_j} \quad (1)$$

where  $n_j$  = the number of cycles applied at load level  $S_j$ ,

and  $N_j$  = the number of cycles required to cause fatigue failure at the same load level  $S_j$ ,  
with failure occurring when  $D = 1$ .

### 2.3 Wind Induced Fatigue of Metal Roof Claddings

This section discusses the above topic in relation to roof claddings based on Walker (1984). Cyclonic winds cause the light gauge metal roof claddings to fail in fatigue because they are fluctuating due to turbulence induced in the flow caused by interaction with the structure and wind induced vibration of the structure or structural components. It is considered that situations in which fatigue failure may occur are generally characterized by metallic structural components, stress concentrations and large number of repeated moderate to high loads. When metal roof claddings are subjected to cyclonic winds, all these three situations prevail and thus make these claddings susceptible to fatigue damage.

Two categories of structures can be identified with regard to wind induced fatigue. The first category is known as static structures, in which the structure or structural component responds directly in a static manner to the fluctuating wind pressure loading without any significant inertial effects and is characterized by high natural frequency and/or large material damping. Light roof claddings fall into this category. The second category of dynamic or aeroelastic structures is that group in which dynamic excitation of structures or structural elements occurs due to fluctuating wind pressure.

Fatigue failure during cyclonic winds also depends on the fatigue loading characteristics of the wind pressure such as the characteristics of the wind climate, the location of the components in the structure and the tributary area exposed to wind pressure supported by the component. Wind pressure records on model and full scale houses reveal that roof claddings have a greater susceptibility to fatigue failure than the structural elements resisting windward wall pressure and this indicates the importance of location of structure. With regard to tributary area, elements with small tributary area such as roof cladding connections are likely to be more at risk than those with large tributary area such as the connections between roof trusses and walls.

Only severe wind events such as cyclones can cause a fatigue failure. For fatigue failure to occur the stresses induced have to be above the fatigue limit and the event has to last for a considerable time to cause sufficient cycles of loading. Consequently, commonly occurring wind conditions or even extreme wind conditions of thunderstorms or tornadoes which are of short duration may not cause fatigue failures.

In summary from all viewpoints the light gauge metal roof cladding connections could suffer fatigue damage when subjected to cyclonic winds unless they are designed for such events.

## **2.4 Fatigue Investigations on Corrugated Roof Claddings**

Fatigue investigations on roof claddings were first conducted by Beck and Morgan (1975) and Morgan and Beck (1977). Their laboratory and field investigations revealed that fatigue failure at the sheet fixings caused the widespread roofing damage during cyclone Tracy.

Beck (1978) and Beck and Stevens (1979) continued this investigation further by testing a large number of roof claddings using constant amplitude and programmed loading tests. A two-span roofing assembly of 650 mm span with simply supported ends was used in the investigation. Roofing was fastened with four screws across the width using a three fasteners per sheet arrangement. Constant amplitude load tests were used to determine the factors influencing the fatigue failure. Their results confirmed that the intensity of loading due to cyclone Tracy could cause fatigue failure of screw-fixed corrugated roof claddings. They concluded that the DABM test was too conservative and recommended the use of TR440 loading sequence and the more complicated programmed loading sequence they had developed.

Neal (1984) carried out tests on corrugated steel roof claddings (New Zealand Fletcher Brownbuilt's galvanized roofing) which were nail-fixed at alternate crests. Only two nails were used in Neal's laboratory model which was constructed to model an actual span of 1200 mm as described by Reardon (1980). He observed localized plastic deformation of the sheet to occur at the fastener heads at loads less than the allowable load per fastener based on nail withdrawal strength. It was concluded that roofing may suffer fatigue failure when subjected to repeated loading above the local plastic buckling load. It was recommended that the allowable design load per fastener for use with 50 year return design wind loads should not exceed 550 N.

In Slogrove's (1985) investigation roofing specimens were screwed at alternate crests with four screws across the width and represented an actual internal span of 1040 mm according to Reardon (1980). He concluded that localized buckling around the fasteners is the cause of low cycle fatigue cracking and that any cyclic loading through this local buckling tends to induce fatigue failure. These conclusions were in agreement with those of Neal (1984). Comments were also made on the adequacy of the current fatigue testing methods.



## 2.5 Simulation of Wind Fatigue Loading

Fatigue testing can be conducted to achieve a variety of objectives, for example, to determine the basic material fatigue data, or the performance of design details or the complete structure to resist a certain design event (Mann, 1974). The history of fatigue testing has been essentially characterized by simple constant amplitude sinusoidal loading. However, with the advancement of high-technology fatigue testing machines, realistic testing methods, namely programmed loading tests, random block load tests and random load tests, are currently being used for various fatigue testing purposes.

There are currently two accepted fatigue loading tests for roof claddings, DABM (DRC, 1976) and TR440 (EBS, 1978). The DABM test was introduced soon after cyclone Tracy devastated Darwin. This test consists of 10,000 cycles from zero to design load followed by an overload static test to 1.8 times the design load. As this constant amplitude load test was considered to be too conservative, the TR440 test was developed subsequently. The TR440 test consists of a simple programmed loading sequence as follows:

8000 cycles at 0.625 Design Load (DL)

2000 cycles at 0.75 Design Load

200 cycles at 1.0 Design Load

Overload static test to  $g \times DL$  where  $g$  depends on the number of tests.

At present an extensive investigation is under way at James Cook University to review these fatigue tests to determine whether they are in fact simulating the cyclonic winds or not.

## 3. EXPERIMENTAL METHOD

### 3.1 General

All fatigue tests were conducted using identical test specimens and test set-up to those used earlier for static tests (Mahendran, 1988b). Although complete details of test specimens and test set-up were presented in that report, the following sections present them again for the sake of completeness of this report.

### 3.2 Simulation of Wind Loading

It is to be noted that roof claddings in fatigue fall into the category of static structures. As such a dynamic response analysis of roof claddings is not needed in this investigation.

Roof claddings are predominantly subjected to uplift wind loading which is due to the combination of external and internal wind pressures, both of which fluctuate continuously and largely independently during a tropical cyclone. It is well known that typical wind pressure

loading on roof claddings is a random process. Realistic testing of full scale multi-span roofing assemblies subjected to realistic wind pressure loading is neither practical nor a necessity. Simple laboratory models are in general adequate.

The end spans of a roof cladding are generally subjected to greater suction forces during cyclonic winds. The analysis of a multi-span roofing assembly indicates that the second support from the eaves is very often critically loaded when subjected to wind pressure loading. As the overall problem is somewhat a localized one in the region around the fastener holes, the loading in that region due to bending moment and the concentrated tensile load in the fasteners should be modelled correctly. Hence a two-span roofing assembly with simply supported ends representing an end span was chosen to model the critical regions (second support conditions) of a multi-span roofing assembly.

Midspan line loading was chosen due to practical limitations associated with the use of a commercial hydraulic testing machine. As uniform pressure loading was not used, it was necessary that the main loading parameters at the critical central support, namely the load per fastener and the bending moment were modelled correctly. Hence a number of equivalent test spans of 250 (short span), 500, 650 (medium spans) and 1000 mm (long span) were selected in order to include a wide spectrum of recommended spans of corrugated roofing as in the static investigation, and to test the roofing to various combinations of the two important loading parameters. These laboratory test spans are equivalent to prototype end spans of approximately 350, 700, 900 and 1400 mm, respectively, which are subjected to uniform pressure loading. In the following sections of this report, only the laboratory test span values are mentioned.

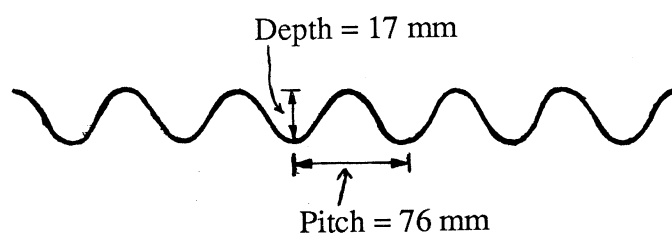
Although typical wind pressure loading on roof claddings is a random loading, only constant amplitude cyclic loading tests from zero or nonzero minimum load to various predetermined maximum loads were conducted as it was believed that these simple tests could provide the necessary information on the basic fatigue behaviour of corrugated roof claddings. It is anticipated that a realistic variable amplitude cyclic loading either as a program load test or a random load test will be considered later as part of the project to review current standard fatigue testing methods.

### 3.3 Test Specimen

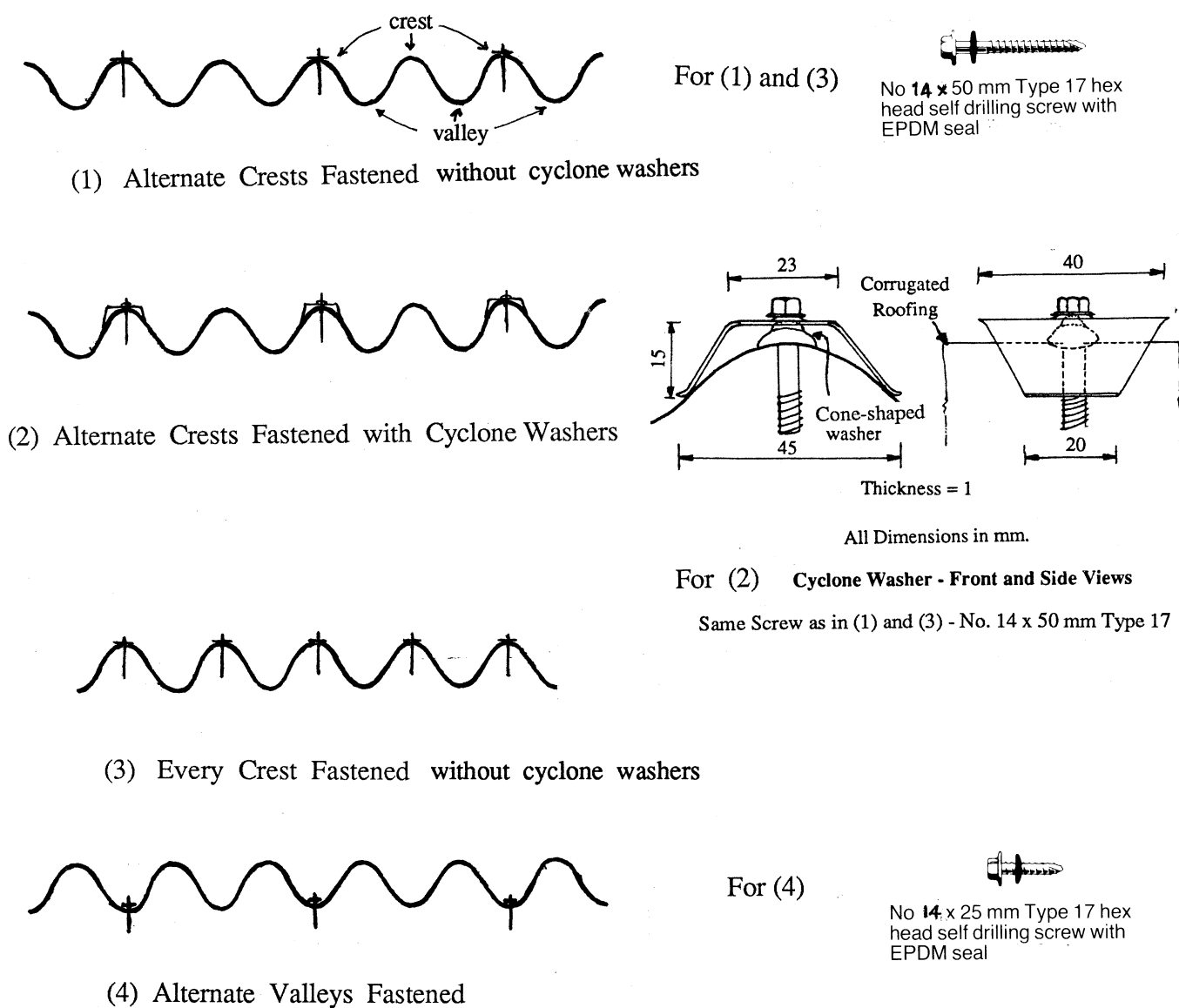
All the fatigue tests were conducted on Lysaght Building Industries' Custom Orb corrugated steel roofing of 0.42 mm base metal thickness (bmt) and 0.47 mm total coated thickness (tct). The corrugated roofing is roll-formed according to AS 1445 (SAA, 1977) from a Zinalume-coated high tensile steel sheet which complies with grade G550 - AZ150 in AS 1397 (SAA, 1984) (i.e., minimum yield stress of 550 MPa and minimum coating mass of 150 g/m<sup>2</sup>). The basic dimensions of the corrugated roofing profile are shown in Figure 2.

Base Metal Thickness = 0.42 mm

Total Coated Thickness = 0.47 mm



Std. Sheet width = 760 mm cover with 1.5 corrugation side laps

**Figure 2. Basic Dimensions of Corrugated Roofing Profile****Figure 3. Test Specimens with Different Fastening Systems**

All the roofing specimens in both the previous static investigation and the current fatigue investigation were rolled from the same coil of steel. Tensile tests were carried out on this coil of steel at the beginning of the static investigation (Mahendran, 1988b). Their results indicated that the strength of the sheet material is satisfactory as the mean yield stress was found to be 690 MPa. However, there was some concern about the very low measured ductility, 0.5%, as AS1397 (1984) specifies a minimum of 2% ductility. Tensile tests on specimens cut from the crests and sides of the corrugated roofing indicated that cold rolling did not alter the original material properties.

Test specimens were fastened using four different fastening systems, namely alternate crest fastening with or without cyclone washers, every crest fastening without cyclone washers and alternate valley fastening (see Figure 3). The manufacturers of corrugated roofing recommend alternate crest fastening with or without cyclone washers for the use in cyclonic areas (LBI, 1987). Alternate crest fastening is referred to in their reference manual as a fixing arrangement with five fasteners per sheet. Every crest fastening is not recommended at all, but alternate valley fastening is recommended for walls. In this investigation, the fastening systems other than those recommended by LBI were also used in order to study the dependence of the fatigue behaviour of corrugated roofing on such fastening systems.

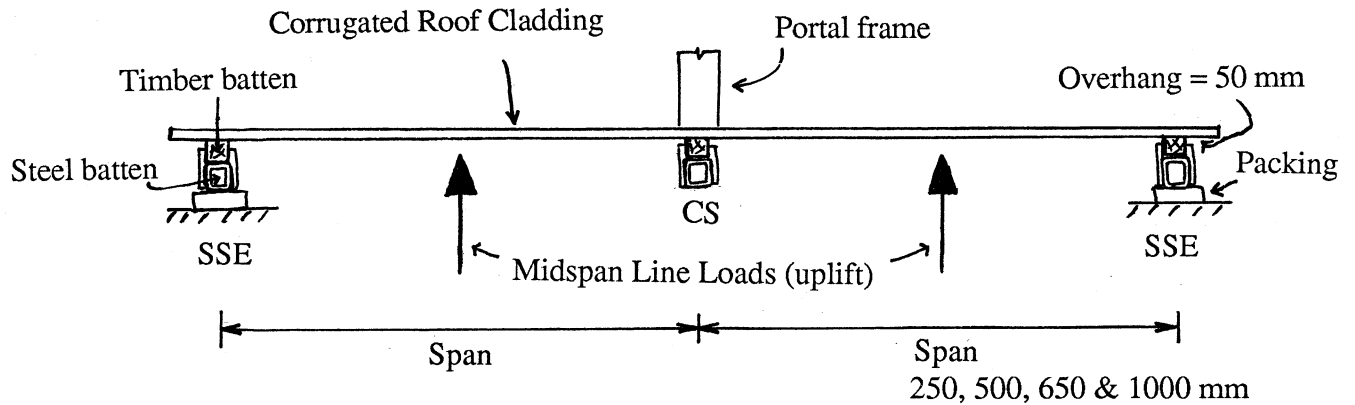
Due to physical constraints of the testing machine, the specimens were only six or eight corrugations wide. It is assumed that the absence of lateral continuity of roofing would have caused very little effect on the fatigue test results. All the test specimens fastened at alternate crests or valleys had three fasteners (six corrugations wide), but in the case of 650 mm span, four fasteners (eight corrugations wide) were mostly used. Five fasteners were used when the specimen was fastened at every crest (see Figure 3).

An overhang of 50 mm was provided on either side of the end supports of the roofing assembly for all the spans. In most cases, the roof sheeting was secured to timber battens with No.14 x 50 mm Type 17 hexagonal head self drilling screws with EPDM seals as recommended by LBI (1987). Shorter screws (25 mm) were used in the case of valley fastening. High quality timber was used in all the tests to prevent premature screw withdrawal from timber. Timber battens were fixed within steel battens and acted as very stiff supports. Although flexible battens or purlins are used in practice, it was decided to use stiff supports such that the effects due to the flexibility were absent in this investigation.

The location and tightening of screws would affect the number of cycles to failure in a fatigue test. Thus all screws were tightened until the neoprene washers were just prevented from rotating to avoid either overtightened or loose screws. Attempts were made to ensure that all the screws were located exactly at the centre of the crest or valley, and perpendicular to the plane of roofing.

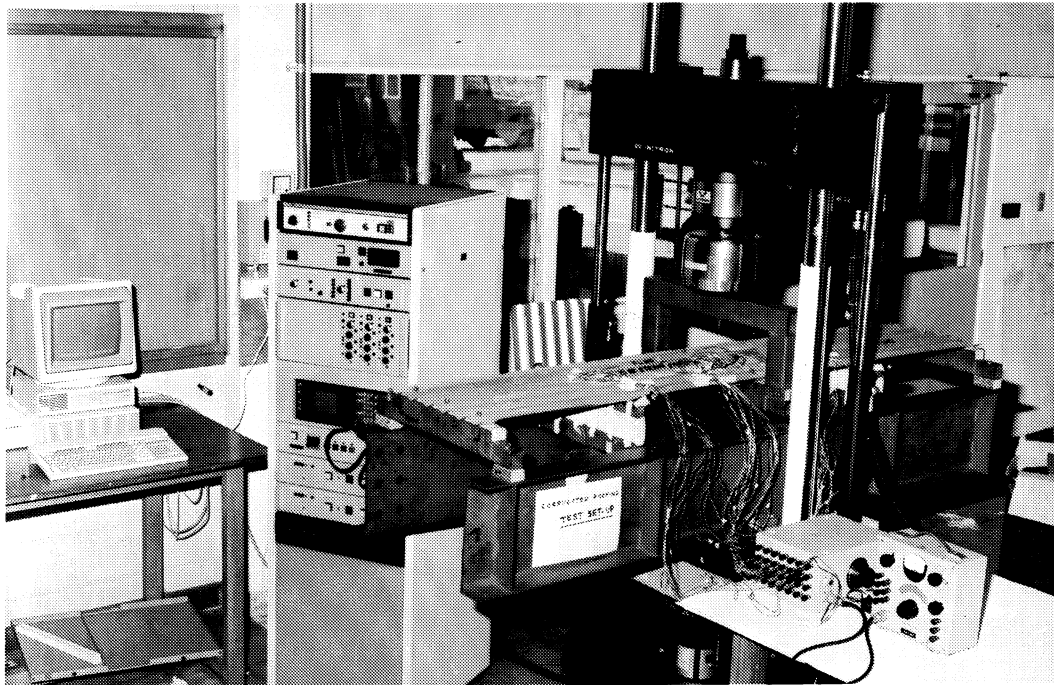
### 3.4 Test Set-up

All tests were conducted on a servo-controlled hydraulic testing machine (Instron) of 100 kN dynamic capacity at the James Cook University Structures Laboratory. A microcomputer HP9122 controlled all the fatigue tests via an intelligent interface. Figure 4 shows the test set-up.



CS : Central Support (supported by portal frame above)  
 SSE : Simply Supported Ends (supported by channel beams)

(a). Line Diagram Illustrating the Test Set-up



(b). Overall View of the Test Set-up for Roofing of 1000 mm Test Span

Figure 4. Test Set-up

Extreme care was taken to ensure that the line loading system applied pressure uniformly to the underside of the corrugations in both their normal and distorted profiles at each midspan. For this purpose a thin rubber tube filled with water was used on top of a rubber pad of width 30 mm that was moulded in the shape of the roofing profile.

A small portal frame supported the central batten against the load cell above it (see Figures 4 and 5) and thus the total reaction force at the central support was directly read from Instron's load display unit at any stage of load cycling. The average load per fastener was obtained by dividing the total reaction force by the number of fasteners at the support. The maximum total reaction at the central support during any fatigue test was less than 10 kN. Therefore the Instron load cell was calibrated carefully using a mercury proving device for a load range from zero to 10 kN and was found to be satisfactory.

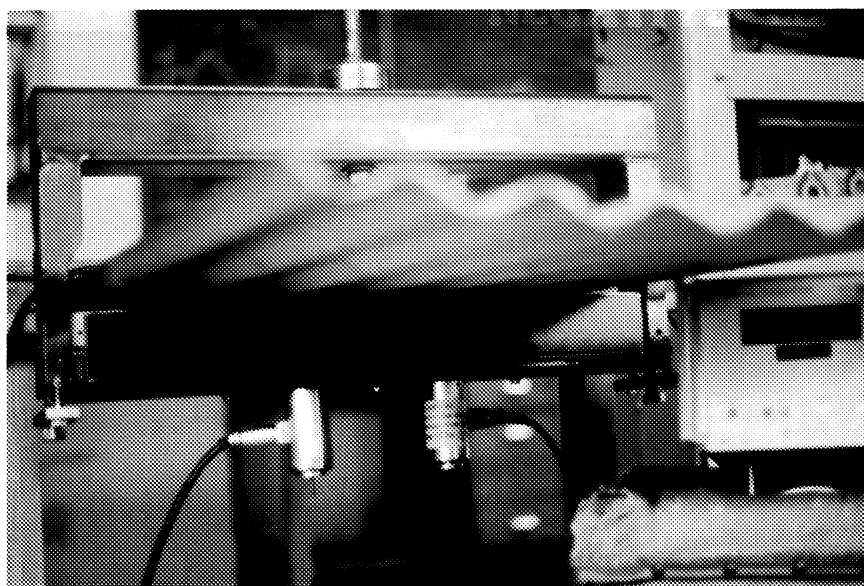


**Figure 5. Measurement of Load in Individual Fasteners**

The average tensile load per fastener was the controlling parameter for all tests and in fact has been the only load measurement during most of the fatigue tests. However, in some tests actual loads in individual fasteners at the central support were measured to verify the assumption of uniform distribution of loading among the fasteners. This uniformity of loading among the fasteners is critical as otherwise fatigue failure will occur prematurely at the fastener which has the greatest load and will not relate to the average load per fastener. Figure 5 shows the arrangement in which the load in each middle fastener at the central support was measured by a tiny load cell. These highly sensitive load cells of 5 kN capacity were designed and made at the Cyclone Testing Station for this specific purpose. The extra-long middle fasteners used for this

purpose were of the same diameter as the usual fasteners and were installed after pre-drilling with the usual fasteners. Results from these tests showed that when the current test set-up with loading pads and water-filled rubber tubes was used, the maximum difference between the actual load in any one of the fasteners at the central support and the average load per fastener obtained from the Instron's load display unit was less than 10% and this was considered satisfactory.

Although only one of the main loading parameters, the average load per fastener at the central support 'P' (in Newtons) was used to control the tests in this fatigue investigation, the other parameter, the bending moment (in Newton-metres) per metre width of roofing 'M' could be determined for each test by the following simple equations obtained by analysing the two-span roofing assembly of span 'L' (in metres).

$$\text{For alternate crest or valley fastening,} \quad M = 0.90 P L \quad (2 a)$$

$$\text{For every crest fastening,} \quad M = 1.80 P L \quad (2 b)$$

### 3.5 Types of Tests

In general there were two types of tests, namely tests with zero minimum load and those with nonzero minimum loads for various preset maximum loads. For tests which were conducted to achieve the first objective of gaining a better understanding of the basic fatigue behaviour of corrugated roofing, load was always cycled from a zero minimum load to various maximum loads. These maximum loads were selected arbitrarily to include a wide spectrum of loading up to the ultimate static failure load for tests on each span of roofing. This first series of tests was conducted for roofing with all four fastening systems and different spans whereas the second series of tests was conducted only on a test span of 650 mm fastened at alternate crests.

The second series of tests was conducted to develop the data base of fatigue characteristics of roof cladding required for the ongoing investigation on the review of current fatigue testing methods. The research methodology of this investigation is described in Jancauskas et al. (1989). Wind tunnel records of roof pressure were used to develop a fatigue wind loading spectrum for a design wind event - a model cyclone. This fatigue wind loading spectrum in a matrix format consists of the number of loading cycles for various combinations of range (0.05 to 1.25) and mean level of loading (0.05 to 0.95) expressed as a ratio of ultimate design wind load. This fatigue wind loading data has to be integrated with the fatigue characteristics of roof cladding system to be obtained from this investigation (second objective). For this purpose, both set of data should relate to the same range and mean levels of loading, and accordingly, the maximum and minimum cyclic loads for the second series of tests were determined using the current working design load per fastener of 550 N used by the manufacturer of corrugated roofing and a factor of 1.5 to convert the working design load to ultimate design load.

### 3.6 Testing Method

A haversine waveform was adopted for all tests. During the early tests a loading frequency of 1.5 Hz was used, but later a smaller frequency of 1.0 Hz was used because cyclic loading of a flexible specimen such as this roofing assembly was made easier at the latter lower frequency. The loading frequency was held constant for any given test, and in most cases for any given group of tests.

All tests were conducted by controlling displacement rather than force. This was necessary for two reasons. Firstly, servo-controlled testing machines are designed for the load control of stiff tension or compression specimens, rather than flexible bending specimens such as corrugated roofing. It should also be noted that the maximum cyclic load encountered during these tests was only 10% of the dynamic capacity of the load cell supplied with the machine. Hence it was found that machine's internal settings could not be adjusted satisfactorily to obtain an optimum performance unless the test was done slowly at frequencies of the order of 0.1 Hz. Secondly, when the specimen began to crack, the loss of specimen's stiffness necessitated readjustment of the machine's internal settings during the test if the same preset maximum and minimum cyclic loads had to be maintained. This readjustment would have to be carried out continuously until failure as the specimen lost its stiffness gradually with increased cracking.

A computer program "FMAXMIN" was written for the case of cyclic waveforms on displacement control for which preset maximum and minimum (peak) cyclic loads were always maintained until failure by updating the peak loads every four cycles. Initially every specimen was loaded statically to the preset maximum cyclic load in order to obtain the required positions of actuator at the preset peak loads. These position data were input into the program along with other data regarding the preset peak loads in kilonewtons, loading frequency, type of waveform and a parameter to relate the position data of actuator to load. This last input parameter, an approximate rate at which the position data of the actuator had to be changed to enable a change of unit load, was obtained from the preliminary static tests for each combination of a particular span and fastening system. When the program was run and the ready button on the machine pressed, cycling was done to the preset position data of the actuator. If this movement of the actuator did not create the required preset peak loads within 0.05 kN, the program reset the position data of actuator until the difference between the actual and the preset peak loads was less than 0.05 kN. Usually in most tests this was achieved within the first ten cycles. The program displayed the peak loads and the number of cycles completed after every cycle in addition to the input data. During testing, obviously, the position data of the actuator should be changed as specimen began to lose its stiffness. The computer program reset the position data of actuator until the difference between the actual and the preset peak loads was less than 0.05 kN. If at any



time during testing the difference between actual and preset peak loads exceeded 0.25 kN, load cycling was terminated automatically.

Attempts were made to record the number of cycles at which crack initiation  $N_i$  occurred in each test. This was a difficult task as an observable crack has to be at least a few millimetres long on the external side of roofing before it is visible to the naked eye. The nature and location of cracking and how they were propagating were observed in each test. Test was continued through crack propagation stages until one or more fasteners pulled through the roofing. First appearance of a visual crack was not considered the failure criterion as it would be too conservative. Instead the disengagement of roofing was considered the fatigue failure. In tests with cyclone washers, tests were continued until the entire cyclone washer-fastener assembly pulled through the roofing. Soon after the occurrence of the fatigue failure, the computer detected the sudden drop in peak loads below the preset peak loads by more than 0.25 kN and thus stopped further cycling. The number of cycles to failure  $N_f$  from the computer's display, the crack type and the failure location (central or edge holes at the central support) were noted for each test.

## 4. RESULTS AND DISCUSSION

### 4.1 General

In this section all the fatigue results obtained for different fastening systems and spans are presented separately and discussed in detail. Attempts are made to correlate the fatigue test results with the results from the static investigation reported earlier (Mahendran, 1988b). To avoid repetition, the reference to the above report is not always made, but simply referred to as static analysis or static investigation.

Some test specimens were inspected for the presence of cracks due to drilling before cyclic loading. No crack or crack-like defect was found before cyclic loading, but cracking initiated and propagated till failure in all cases of roofing of different spans and fastening systems after a certain number of cycles depending on the load levels.

For most tests the number of cycles to crack initiation  $N_i$  was observed and is reported in this section. However, it should be considered as an upper bound because in most cases crack initiation was not detected exactly, but later when it was visible to the naked eye on the surface of roofing.

## 4.2 Roofing Fastened at Alternate Crests without Cyclone Washers

### 4.2.1 Cycling from zero minimum load

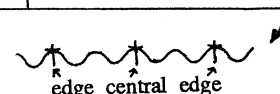
Tables 1 (a) to (d) present the results in this case for test spans of 250, 500, 650 and 1000 mm in that order. All these results are also presented as a fatigue curve of average maximum cyclic load per fastener  $P_{max}$  versus number of cycles to failure  $N_f$  for each span in Figure 6 (a) in which only  $N_f$  is plotted on a  $\log_{10}$  scale. In Figure 6 (b) only the results for the test span of 650 mm are plotted with both axes on a  $\log_{10}$  scale. In both figures the fatigue data appear to fit straight lines quite well. Some of these results have already been presented in Mahendran (1988a,b) and Mahendran and Reardon (1988), but are presented again in this report for the sake of completeness.

**Table 1      Fatigue Test Results of Corrugated Roofing**  
**Fastened at Alternate Crests without Cyclone Washers**

(a) Test span = 250 mm (short span)

Loading Frequency = 1.5 Hz

Cyclic Load Range (N/f)	Number of Cycles to		Type of Crack	Pull Through at
	Crack Initiation $N_i$	Failure $N_f$		
(1) 0 - 350	16,200	117,900	B	Edge Hole
(2) 0 - 400	11,810	44,100	B	Edge Hole
(3) 0 - 425	4,800	16,000	B	Central Hole
(4) 0 - 450	2,200	7,600	B	Central Hole
(5) 0 - 450	1,600	3,500	A-B	Edge Hole
(6) 0 - 500	1,520	3,030	A-B	Edge Hole
(7) 0 - 550	1,350	3,250	A-B	Central Hole
(8) 0 - 650	950	1,750	A	Central Hole
(9) 0 - 800	200	1,250	A	Edge Hole
(10) 0 - 1000	230	800	A	Central Hole
(11) 0 - 1250	190	560	C	Edge Hole

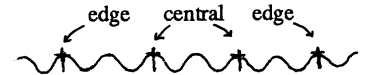


(b) Test span = 500 mm (medium span)

Loading Frequency = 1.5 Hz

Cyclic Load Range (N/f)	Number of Cycles to		Type of Crack	Pull Through at
	Crack Initiation $N_i$	Failure $N_f$		
(1) 0 - 375	n.o.	284,660	B	Central Hole
(2) 0 - 400	5,000	23,920	B	Edge Hole
(3) 0 - 400	7,200	27,470	B	Edge Hole
(4) 0 - 450	2,000	9,090	B	Edge Hole
(5) 0 - 500	n.o.	2,930	B	Edge Hole
(6) 0 - 550	600	1,600	B	Edge Hole
(7) 0 - 600	500	1,440	B	Edge Hole
(8) 0 - 650	160	1,010	A-B	Edge Hole
(9) 0 - 650	100	520	A	Edge Hole
(10) 0 - 800	100	780	A	Central Hole
(11) 0 - 1000	80	430	A	Central Hole

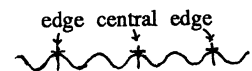
Table 1. Continued



(c) Test span = 650 mm (medium span)

Loading Frequency = 1.0 Hz

Cyclic Load Range (N/f)		Number of Cycles to Crack Initiation $N_i$ Failure $N_f$		Type of Crack	Pull Through at
(1)	0 - 300	n.o.	362,200	B	Edge Hole
(2)	0 - 325	110,000	290,140	B	Edge & Central Holes
(3)	0 - 344	n.o.	274,150	B	Edge Hole
(4)	0 - 350	22,000	62,750	B	Central Hole
(5)	0 - 350	n.o.	320,450	B	Edge Hole
(6)	0 - 375	n.o.	102,200	B	Central Hole
(7)	0 - 387	n.o.	68,650	B	Edge Hole
(8)	0 - 400	n.o.	18,160	A-B	Central Hole
(9)	0 - 400	n.o.	38,710	B	Central Hole
(10)	0 - 413	n.o.	30,210	B	Central Hole
(11)	0 - 413	n.o.	52,150	B	Edge Hole
(12)	0 - 425	n.o.	38,580	B	Edge Hole
(13)	0 - 450	7,000	15,600	B	Edge Hole
(14)	0 - 475	n.o.	7,780	Almost B	Central Hole
(15)	0 - 500	n.o.	4,420	A-B	Central Hole
(16)	0 - 525	n.o.	3,840	A-B	Edge Hole
(17)	0 - 550	700	2,250	A-B	Central Hole
(18)	0 - 600	500	1,560	A-B	Central Hole
(19)	0 - 650	120	650	A	Edge Hole
(20)	0 - 700	80	610	A	Central Hole
(21)	0 - 800	60	430	A	Central Hole
(22)	0 - 1000	60	340	A	Both Central Holes



(d) Test span = 1000 mm (long span)

Loading Frequency = 1.5 Hz

Cyclic Load Range (N/f)		Number of Cycles to Crack Initiation $N_i$ Failure $N_f$		Type of Crack	Pull Through at
(1)	0 - 275	130,000	349,830	B	Edge Hole
(2)	0 - 300	32,300	68,100	B	Central Hole
(3)	0 - 350	n.o.	39,700	B	Central Hole
(4)	0 - 375	6,000	20,920	B	Edge & Central Holes
(5)	0 - 400	1,900	9,040	B	Central Hole
(6)	0 - 450	1,300	3,990	B	Edge Hole
(7)	0 - 450	800	1,950	A-B	Central Hole
(8)	0 - 500	200	950	A-B	Central Hole
(9)	0 - 550	250	880	Almost A	Central Hole
(10)	0 - 650	200	720	A	Central Hole
(11)	0 - 800	70	540	A	Edge & Central Holes

Note 1. n.o. - Crack initiation was not observed in this test.

2. N/f - Newtons per Fastener

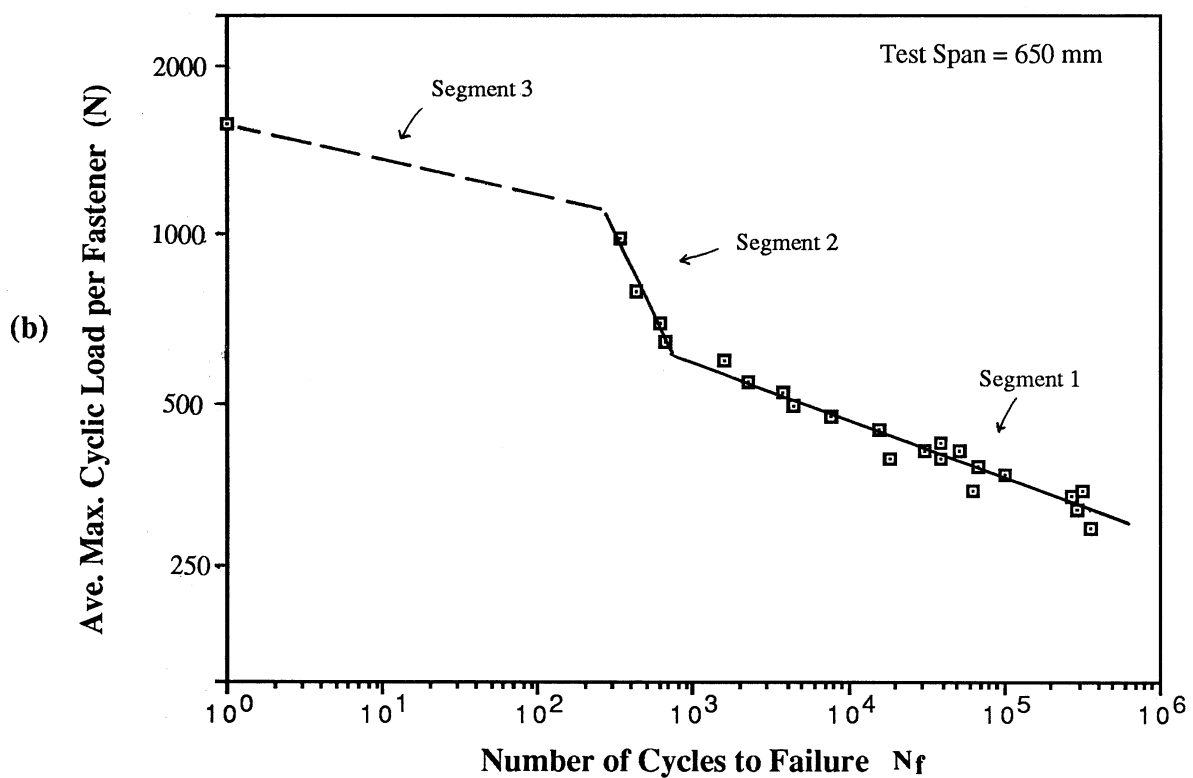
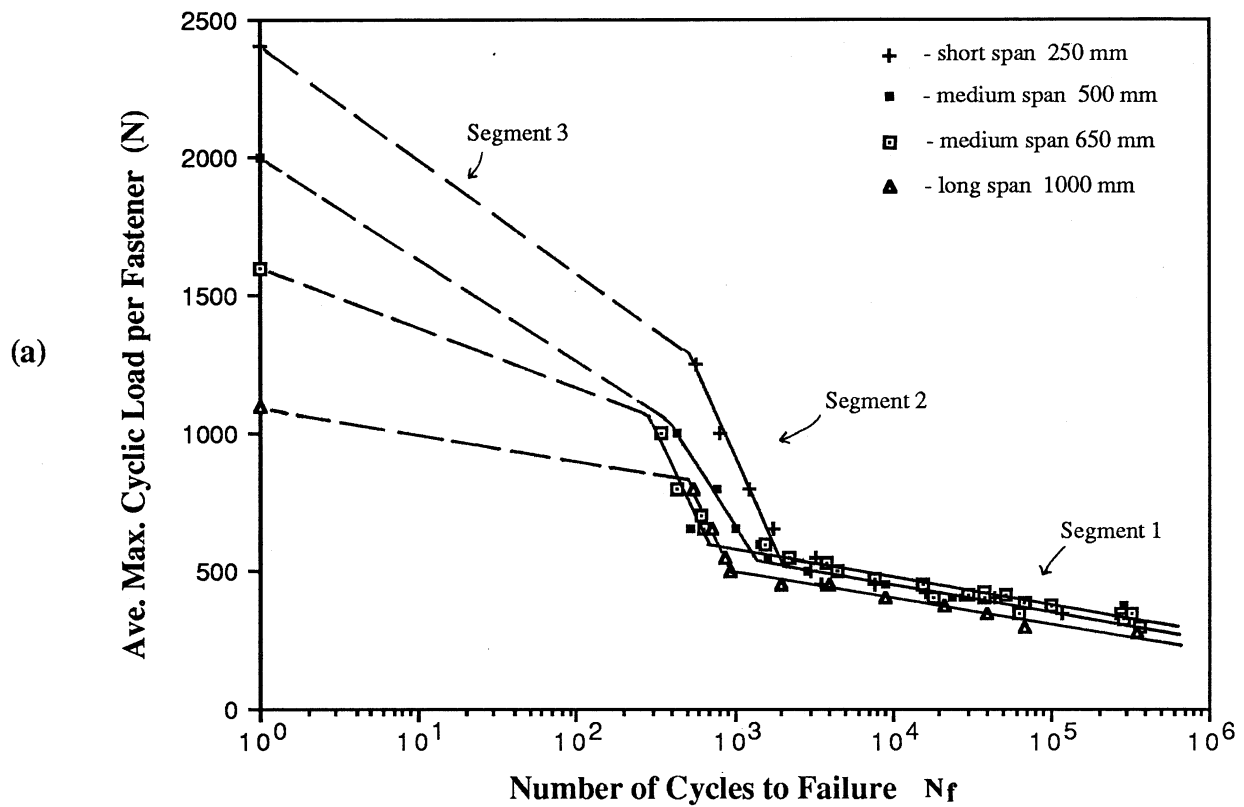


**Figure 6. Fatigue Curves for Corrugated Roofing Fastened at Alternate crests without Cyclone washers (Cycling from zero minimum load)**

Results from a static investigation (Mahendran, 1988b) are in excellent correlation with the fatigue test results and thus explain the fatigue behaviour quite well. The static tests revealed the occurrence of local plastic deformations associated with buckling (LPD) at approximately the same load per fastener (550 to 650 N) for all the test spans of 250, 500, 650 and 1000 mm. For a bending test the resulting load-deflection curve was quite unusual with four loading stages (see a similar curve in Figure 13 later), namely the initial loading stage up to the LPD load (stage 1), the LPD stage (stage 2), the loading beyond the LPD load (stage 3), and the collapse by buckling and yielding of the entire cross-section at midspans and central support (stage 4). Accordingly, the fatigue curves for all the spans of roofing have different segments as shown in Figures 6 (a) and (b). Segment 1 corresponds to the stage 1 loading of static test up to the LPD load whereas Segment 2 corresponds to the loading into stages 2 and 3. Segment 3 corresponds to very high loading closer to ultimate static failure load which led to a static failure by buckling and yielding at midspans before a fatigue failure could occur. Hence Segment 3 cannot be considered as part of the fatigue curve and is shown by a dashed line for each span in Figure 6.

A small region around the fastener hole at the central support was found to have very large stress concentrations from both a finite element analysis and strain-gauged tests, and in fact, the region was yielding at the respective LPD load for each span (Mahendran, 1988b). Confirming this, the same region cracked after relatively small number of cycles during the fatigue tests on all the spans of roofing (see Figure 9 later for cracked region). When the maximum cyclic load  $P_{max}$  approached or exceeded the LPD load, the fatigue performance deteriorated rapidly for all the spans as seen in Table 1 and Figure 6 due to the fact that the same region yielded at the LPD load level. For example, the  $N_f$  was less than 2,000 cycles once  $P_{max}$  was greater than the LPD load for each span.

The use of simple engineering bending theory indicates that the central support crests of this two-span roofing assembly under uplift wind loading is subjected to compressive membrane stresses. This means ideally no fatigue cracks should develop at the crests during fatigue tests. In contrast, the finite element analysis in the static investigation revealed that there were out-of-plane bending stresses in both transverse and longitudinal directions in addition to the membrane compressive stress in the longitudinal direction at these crests due to the large cross-sectional distortion. This analysis showed that there were very large tensile stresses on the bottom surface of roofing at these crests, and these stresses reached yield values at the LPD load for all the spans of roofing. Therefore one would expect the roofing to crack at the bottom surface of the central support crests despite the presence of compressive membrane stress. This was indeed the case in all the fatigue tests. Cracks were first observed on the bottom surface and they developed through the thickness first and then in the plane of roofing. A similar observation was made by Walker and Kwok (1988) in their investigation on damaged steel cylinders. They observed

fatigue cracking due to the presence of large residual tensile stresses caused by denting despite the fact that the cylinders were subjected to cyclic compressive loading.

For the fatigue tests with  $P_{max}$  greater than the LPD load, the preliminary static loading up to the preset maximum cyclic load (first cycle) in every test confirmed the occurrence of local plastic buckling deformation at approximately the same load of 550 to 650 N per fastener (N/f) for all the spans. When local plastic buckling occurred at the central support fasteners on initial loading (first cycle), large diamond shaped dimples formed under the fastener heads and on unloading the cross-section at the central support did not return to its original profile. Therefore a loss of stiffness should have resulted due to this buckling and also due to the associated yielding in the first cycle. Because of this, local plastic buckling occurred at a lower load level on reloading in the second cycle. However, this buckling occurred at the same load level after the second cycle probably because there was no further geometric changes. Figure 7 shows the reduction in LPD load after the first loading cycle for a test span of 650 mm. The LPD load in the second cycle was between 500 and 550 N/f compared to 650 N/f in the first cycle. The LPD load after the second cycle was still found to be between 500 and 550 N/f, however the results of third and fourth cycles are not shown in the same figure for the sake of clarity.

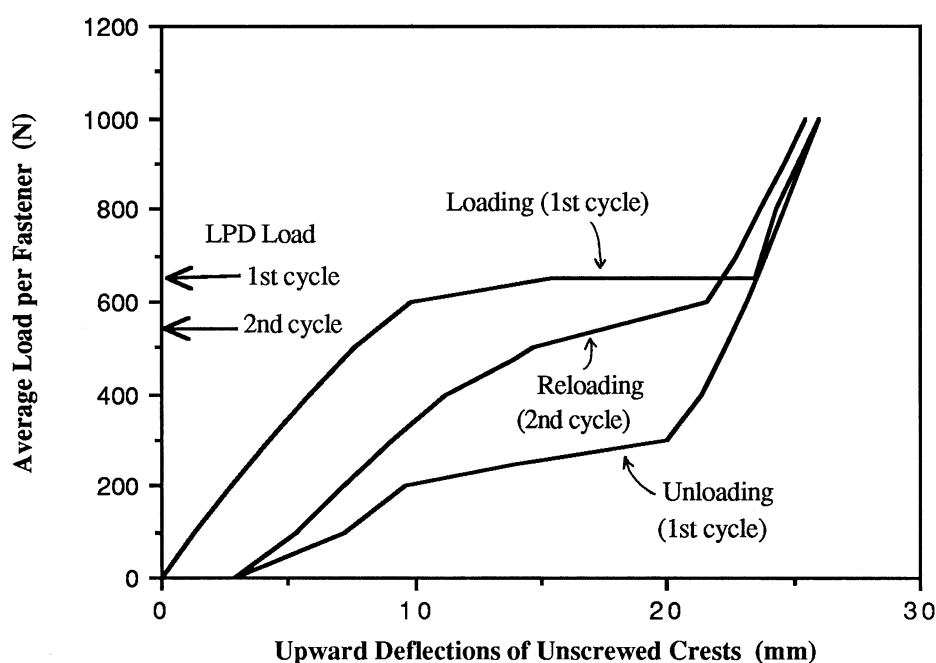


**Figure 7. Reduction in LPD Load with Load Cycling**  
Corrugated Roofing Fastened at Alternate Crests without Cyclone Washers

The presence of reserve static strength beyond the LPD load is of no importance from a fatigue point of view. For example, specimens (test span = 650 mm) representing a common prototype

span of 900 mm failed in fatigue after about 4,000 cycles and after only 650 cycles at 30% and 40% of the ultimate static failure load, respectively. The cracks are likely to develop due to the high stress levels in the vicinity of the fasteners, particularly near and above the LPD load. This explains the commonly observed low cycle fatigue cracking of corrugated roofing. The fact that fatigue failure occurred within 10,000 cycles (in fact, only 2250 cycles) for 650 mm test span at the current design load level of 550 N/f means that the fatigue failure here can be categorized under low cycle fatigue.

Figure 6 (a) shows that Segment 1 of all the fatigue curves are in close proximity which means that the stress levels in the vicinity of central support fasteners causing fatigue cracks are approximately of the same order for all the spans. This was already predicted by the static analysis. The anomalous observation of the occurrence of local plastic buckling deformations at approximately the same load per fastener for all the spans is in agreement with the fatigue test results. It was shown by the static investigation that the greater cross-sectional distortion that occurred for shorter span roofing caused the overall stress levels in the vicinity of central support fasteners to be of the same order for all the spans.

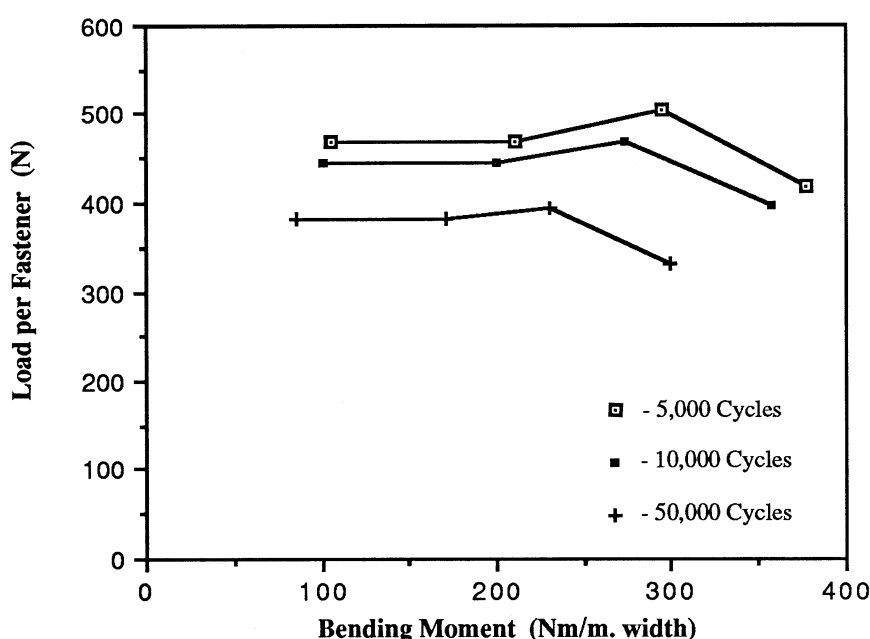


**Figure 8. Effect of Loading Parameters on Fatigue Failure**  
Corrugated Roofing Fastened at Alternate Crests without Cyclone Washers

These results are quite important as they mean that the load per fastener is the most important loading parameter controlling the fatigue behaviour of roofing fastened at alternate crests. This is indeed clearly shown by Figure 8 in which the combination of load parameters, the load per fastener and bending moment at the central support that causes a fatigue failure after 5,000,

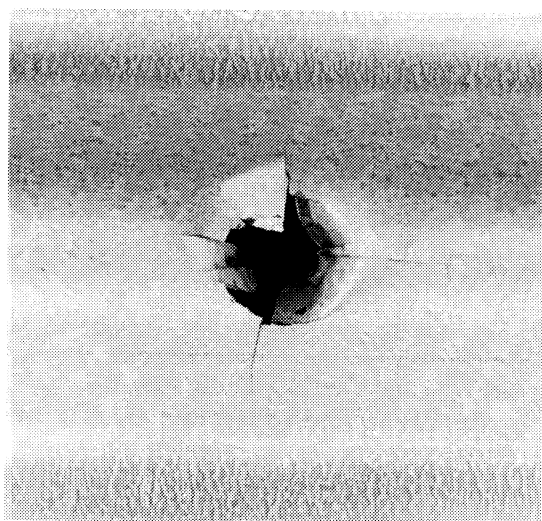
10,000 and 50,000 cycles are plotted using the results from all the four spans. The fact that all the curves are almost horizontal indicates that bending moment at the central support has little effect on the fatigue behaviour. Hence they confirm the current design practice in which the fatigue test results for a single span of roofing are extrapolated to other spans. However, beyond the LPD load, as with the static load-deflection curves, the fatigue curves are not the same for all the spans. This means that both load per fastener and bending moment at the central support are important fatigue parameters above the LPD load, but this deduction may not be so important as the design load should never be greater than the LPD load.

As seen in Table 1,  $N_f$  is always many times greater than  $N_i$ . This means that appearance of a crack on the roofing assembly did not mean an imminent failure. Crack propagation stages contributed significantly to the life of roofing assembly at all load levels.

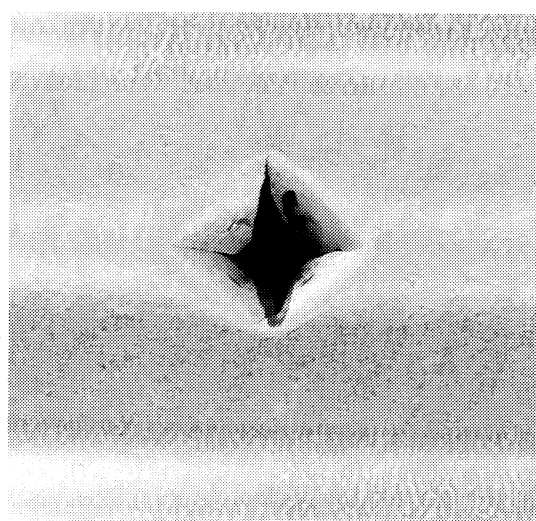
Four different crack types (three of which were commonly observed) were observed for all the spans of roofing. In Segment 1, cracks always initiated from the edge of central support fastener holes and propagated in all directions till the fastener pulled through the roofing. A typical crack (type B) is shown in Figure 9 (a). In Segment 2, due to the fact that load cycling went through local plastic deformation stages, cracks always initiated at points away from the fastener hole and propagated towards the fastener until the fastener pulled through the roofing. A typical crack, type A, in this instance, is shown in Figure 9 (c). The third crack type, referred to as A-B in Table 1, was observed when the maximum cyclic load was approaching the LPD load in Segment 1. In this instance, cracks initiated from the edge of fastener holes and propagated only in the longitudinal and transverse directions as seen in Figure 9 (b). The fourth crack type C shown in Figure 9 (d) was observed only in the short span roofing subjected to very high loads in which the roofing tore around the hole and let the fastener pull through. These cracks were similar to those observed during the investigation on corrugated roofing by Beck and Stevens (1979). However, the  $N_f$  values for nominally the same load per fastener cannot be compared as their results were mainly for roofing fastened by a three fasteners per sheet arrangement.

It is noted that the crack types observed in this series of tests were related to stress levels in the vicinity of fastener holes and thus to  $N_f$ . Crack type B was always associated with larger  $N_f$  whereas type A was associated with smaller  $N_f$  and type A-B with moderate  $N_f$  as seen in Table 1. It is interesting to observe that in Table 1 (c), one of the two tests with a cyclic load range of zero to 400 N/f had a smaller  $N_f$  than the other as it was associated with the formation of type A-B crack instead of type B as in the other test. During Segment 2,  $N_f$  values were relatively smaller and changed little with increasing load. Accordingly, there was little difference among the cracks observed during this segment. However, during Segment 1 as load was increased  $N_f$  decreased significantly and crack type changed from B to A-B as shown in Figure 9.

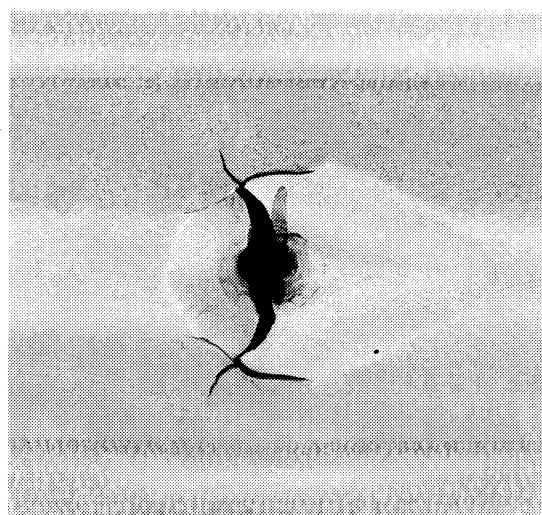




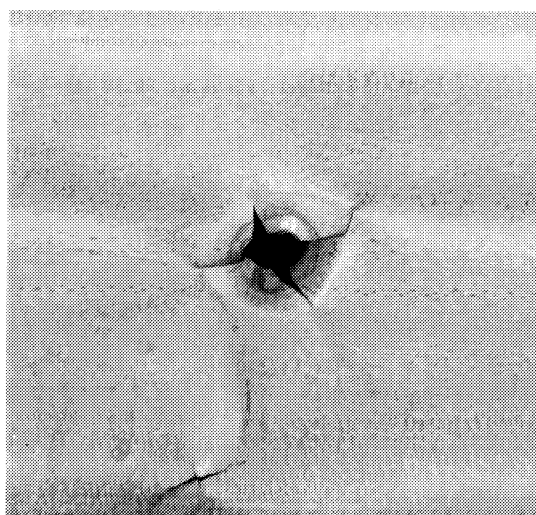
**(a) Type B**



**(b) Type A-B**



**(c) Type A**



**(d) Type C**

**Figure 9. Typical Cracks Observed on Corrugated Roofing  
Fastened at Alternate Crests without Cyclone Washers**

In Table 1 the location at which the fastener pulled through the roofing was also mentioned. As seen from the table, failure was never isolated to one particular location, but randomly to different locations for each test. This is considered a desirable test result as it indicates that the current test set-up or testing method used was not in any way biased to cause failure at one particular location. It also meant that the largest load did not occur at the same location in all tests. It is to be noted that the difference in fastener loads could not have been more than 10% of the average fastener load. This was reflected indirectly by the fact that even though only one fastener pulled through in most cases other adjoining holes were found to have cracked significantly at failure.

Results shown in Figure 6 and Table 1 show a greater scatter of data at lower load levels. This is considered a common observation in fatigue tests, especially on high strength metals. In fact, it is stated that it is not uncommon to find a ratio of longest to shortest fatigue life of 50 or more at the same load level near the fatigue limit (D'Isa, 1968).

For Segments 1 and 2 for the test span of 650 mm shown in Figures 6 (a) and (b), mathematical equations relating  $P_{max}$  and  $N_f$  were derived using the method of least squares. It was found that the fatigue curve in Figure 6 (b) in which both axes were plotted on a log scale provided a better correlation. Therefore only the equations obtained from Figure 6 (b) are presented as follows.

$$N_f = c \cdot P_{max}^{-b} \quad (3)$$

where

$c = 10^{29.3}$	and	$b = 9.47$	for Segment 1 and
$c = 10^{7.5}$	and	$b = 1.65$	for Segment 2.

According to Ekvall and Young (1976), the value of  $b$  for steel ranges from 5 to 7. However, for corrugated steel roofing, this value is 9.47 or 1.65 depending on the load level as seen above.

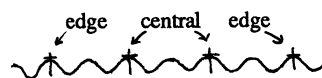
It is to be noted that no attempts were made to determine the fatigue limit. The smallest maximum cyclic load for the test span of 650 mm was 300 N/f and the corresponding  $N_f$  was 362,200 (see Table 1). It was thought that roofing would still crack at a lower maximum cyclic load of 250 N/f if sufficient number of cycles have been accrued. Therefore it was considered that the endurance limit instead of the fatigue limit should be determined. From the fatigue curve in Figure 6 (b), the endurance limit was estimated to be 285 N/f corresponding to an  $N_f$  of  $10^6$  cycles.

#### 4.2.2 Cycling from nonzero minimum load

Results from this series of tests for two test spans of 650 and 1000 mm are presented in Tables 2 (a) and (b), respectively. In the case of 650 mm test span, a large number of tests was conducted under various combinations of range and mean level of loading to produce the fatigue

characteristics of this roof cladding system (see Section 3.5). However, in the case of 1000 mm test span, only a limited number of preliminary tests was conducted. Although the test results for 1000 mm test span have been reported earlier (Mahendran and Reardon, 1988), they are presented again in this section for the sake of completeness. Results in Table 2 (a) are grouped according to crack type, but are presented again in a different format in Table 3.

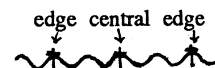
**Table 2      Fatigue Test Results of Corrugated Roofing**  
**Fastened at Alternate Crests without Cyclone Washers**



(a) Test span = 650 mm

Loading Frequency = 1.0 Hz

	Cyclic Load (N/f)		Number of Cycles to Failure $N_f$	Type of Crack	Pull Through at
	Min. - Max.	Range			
(1)	268 - 474	206	325,500	B	Edge Hole
(2)	144 - 433	289	350,200	B	Edge Hole
(3)	227 - 516	289	87,770	B	Edge Hole
(4)	103 - 474	371	42,200	B	Edge & Adj. Central Holes
(5)	351 - 557	206	137,750	A-B	Central Hole
(6)	309 - 598	289	49,540	A-B	Central Hole
(7)	186 - 557	371	15,650	A-B	Central Hole
(8)	62 - 516	454	4,780	A-B	Edge Hole
(9)	144 - 598	454	4,780	A-B	Central Hole
(10)	62 - 681	619	1,400	A-B	Central Hole
(11)	516 - 722	206	178,190	H*	Central Hole
(12)	392 - 681	289	33,470	H*	Both Central Holes
(13)	474 - 763	289	73,590	H*	Central Hole
(14)	557 - 846	289	113,670	H*	Edge Hole
(15)	351 - 722	371	9,650	H*	Both Central Holes
(16)	516 - 887	371	45,080	H*	Central Hole
(17)	227 - 681	454	4,220	H*	Both Central Holes
(18)	309 - 763	454	3,350	H*	Central Hole
(19)	186 - 722	536	3,450	H&H*	Edge & Adj. Central Holes
(20)	268 - 804	536	2,640	H*	Central Hole
(21)	186 - 887	701	1,530	H*	Edge & Adj. Central Holes
(22)	268 - 969	701	2,400	H*	Both Central Holes
(23)	433 - 639	206	52,850	H	Central Hole
(24)	268 - 639	371	10,400	H	Edge Hole
(25)	433 - 804	371	11,920	H	Central Hole
(26)	392 - 846	454	2,650	H	Central Hole
(27)	103 - 639	536	2,240	H	Central Hole
(28)	351 - 887	536	2,670	H	Central Hole
(29)	144 - 763	619	1,690	H	Edge Hole
(30)	227 - 846	619	1,600	H	Central Hole
(31)	309 - 928	619	2,220	H	Central Hole
(32)	103 - 804	701	1,140	H	Central Hole
(33)	144 - 928	784	1,370	H	Edge & both Central Holes
(34)	227 - 1011	784	1,410	H	Central Hole
(35)	186 - 1052	866	1,160	H	Central Hole
(36)	103 - 639	536	1,320	A	Central Hole
(37)	62 - 846	784	890	A	Central Hole
(38)	103 - 969	866	600	A	Central Hole
(39)	62 - 1011	949	400	A	Central Hole

**Table 2. Continued**

(b) Test span = 1000 mm

Loading Frequency = 1.5 Hz

	Cyclic Load (N/f)		Number of Cycles to Failure $N_f$	Type of Crack	Pull Through at
	Min. - Max.	Range			
(1)	125 - 375	250	70,880	B	Central Hole
(2)	125 - 400	275	108,370	B	Central Hole
(3)	125 - 450	325	12,670	Almost A-B	Central Hole
(4)	125 - 500	375	5,640	H	Central Hole
(5)	125 - 650	525	1,700	A	Edge & Adj. Central Holes
(6)	125 - 800	675	650	A	Central Hole
(7)	250 - 400	150	197,550	B	Central Hole
(8)	250 - 450	200	98,500	B	Central Hole
(9)	250 - 500	250	16,900	H*	Edge & Adj. Central Holes
(10)	250 - 650	400	3,870	H*&H	Edge & Adj. Central Holes
(11)	250 - 650	400	4,360	H	Edge & Adj. Central Holes
(12)	250 - 800	550	880	A	Edge & Adj. Central Holes

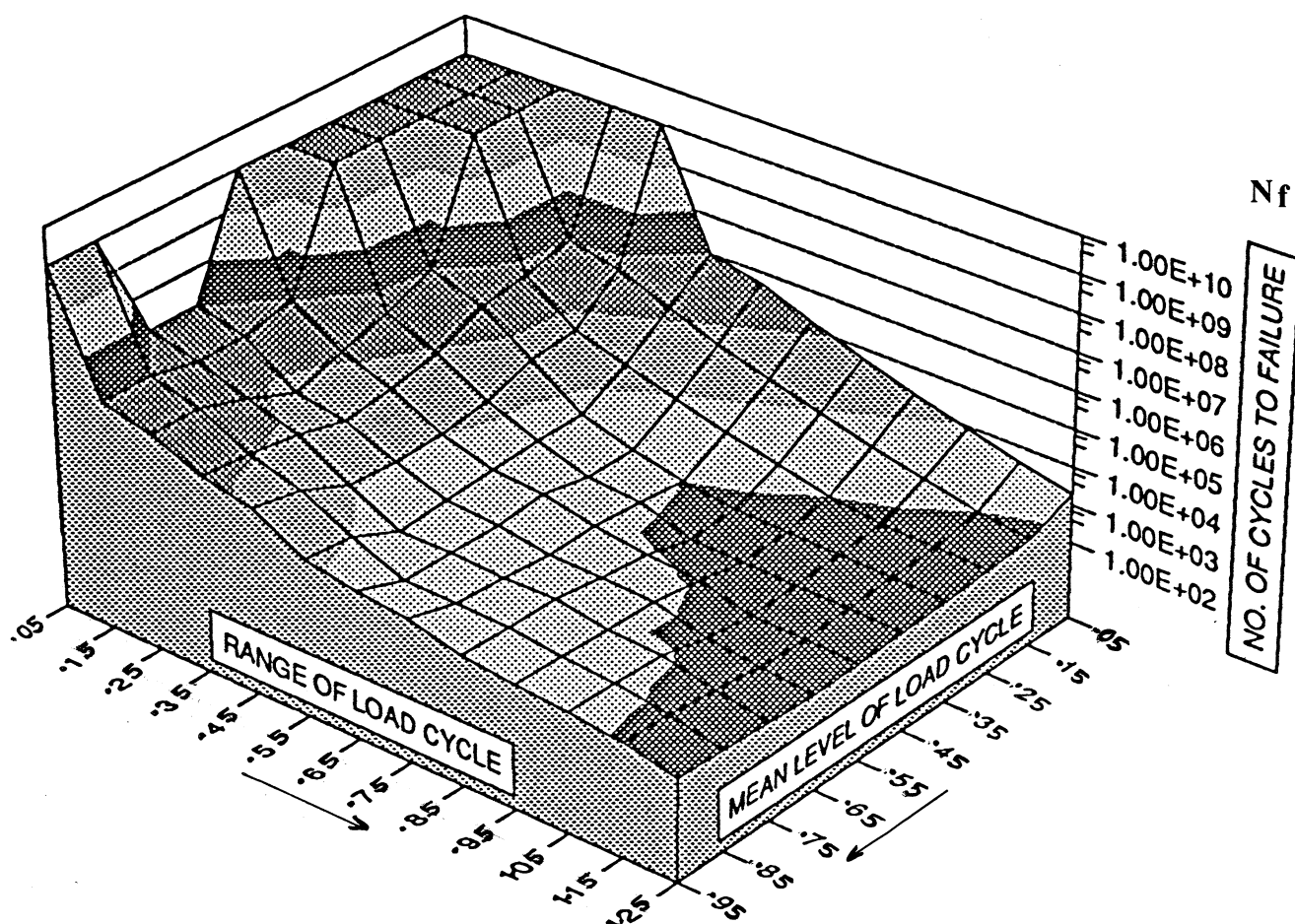
Table 3 presents all the available fatigue test data for the test span of 650 mm in a matrix format as required for the analysis of fatigue characteristics of wind loads. Both range and mean level of loading are given as ratios of ultimate design load ( $P_u$ ) of 825 N. The range of cyclic loading (in Newtons) and the  $N_f$  are given in each square for every combination of range and mean level of loading. When the combination resulted in a negative value for the minimum cyclic load, representing a positive pressure on the roofing, it was taken as zero. This is based on the fact that positive pressure loading on roofing does not cause any fatigue damage. The fatigue equations (no.3) derived earlier in Section 4.2.1 were used to calculate the  $N_f$  for the cyclic loading with zero minimum load in Table 3. For load cycling with a minimum load of 21 N, the same equations were used and it is considered a reasonable assumption. For all other cases with a minimum load greater than 21 N, results were based on a minimum of one actual test. No test was done in the case of obvious infinite cycles category. The maximum  $N_f$  during any test on 650 mm test span was about 360,000. Once a test showed an  $N_f$  greater than 300,000, all other obviously less severe tests were not conducted, but were assigned values of either 500,000,  $10^6$  or  $10^9$ . The assigned value was based on the knowledge of  $N_f$  for other tests in the vicinity of this test. Table 3 includes these values. Figure 10 presents the same information in Table 3 as a three-dimensional plot of cycles to fatigue failure.

Results from this series of tests indicate that not only maximum cyclic load was critical in describing the fatigue behaviour, but also the range of loading. For the same maximum cyclic load  $P_{max}$  of 433 N (less than the LPD load),  $N_f$  increased from about 21,000 cycles to 350,200 cycles when the range was reduced by 144 N. Even when  $P_{max}$  was greater than the LPD load, the same observation was made. For example, for a  $P_{max}$  of 722 N,  $N_f$  increased from a mere 540 to 3,450 cycles when the range was reduced by 186 N.

TABLE 3  
Fatigue Characteristics of Corrugated Roof Cladding  
Load Range per Fastener (N) and Number of Cycles to Failure.

Range / Pu Mean / Pu	(1) 0.05	(2) 0.15	(3) 0.25	(4) 0.35	(5) 0.45	(6) 0.55	(7) 0.65	(8) 0.75	(9) 0.85	(10) 0.95	(11) 1.05	(12) 1.15	(13) 1.25
(1) 0.05	21 - 62 10 <sup>9</sup>	0 - 103 10 <sup>9</sup>	0 - 144 10 <sup>9</sup>	0 - 186 10 <sup>9</sup>	0 - 227 10 <sup>9</sup>	0 - 268 10 <sup>6</sup>	0 - 309 512,970	0 - 351 153,440	0 - 392 53,900	0 - 433 21,010	0 - 474 8,920	0 - 516 3,990	0 - 557 1,940
(2) 0.15	103 - 144 10 <sup>9</sup>	62 - 186 10 <sup>9</sup>	21 - 227 10 <sup>9</sup>	0 - 268 10 <sup>6</sup>	0 - 309 512,970	0 - 351 153,440	0 - 392 53,900	0 - 433 21,010	0 - 474 8,920	0 - 516 3,990	0 - 557 1,940	0 - 598 990	0 - 639 660
(3) 0.25	186 - 227 10 <sup>9</sup>	144 - 268 10 <sup>9</sup>	103 - 309 10 <sup>9</sup>	62 - 351 500,000	21 - 392 53,900	0 - 433 21,010	0 - 474 8,920	0 - 516 3,990	0 - 557 1,940	0 - 598 990	0 - 639 660	0 - 722 540	0 - 804 450
(4) 0.35	268 - 309 10 <sup>9</sup>	227 - 351 10 <sup>9</sup>	186 - 392 10 <sup>6</sup>	144 - 433 350,200	103 - 474 42,200	62 - 516 4,780	21 - 557 1,940	0 - 598 990	0 - 639 660	0 - 722 540	0 - 804 450	0 - 887 390	0 - 969 330
(5) 0.45	351 - 392 10 <sup>9</sup>	309 - 433 10 <sup>9</sup>	268 - 474 325,500	227 - 516 87,770	186 - 557 15,650	144 - 598 4,780	103 - 639 1,780	62 - 681 1,400	21 - 722 540	0 - 763 500	0 - 804 450	0 - 846 420	0 - 887 390
(6) 0.55	433 - 474 10 <sup>9</sup>	392 - 516 10 <sup>6</sup>	351 - 557 137,750	309 - 598 49,540	268 - 639 10,400	227 - 681 4,220	186 - 722 3,450	144 - 763 1,690	103 - 804 1,140	62 - 846 890	21 - 887 390	0 - 928 360	0 - 969 330
(7) 0.65	516 - 557 10 <sup>6</sup>	474 - 598 500,000	433 - 639 52,850	392 - 681 33,470	351 - 722 9,650	309 - 763 3,350	268 - 804 2,640	227 - 846 1,600	186 - 887 1,530	144 - 928 1,370	103 - 969 600	62 - 1011 400	21 - 1052 290
(8) 0.75	598 - 639 10 <sup>6</sup>	557 - 681 500,000	516 - 722 178,190	474 - 763 73,590	433 - 804 11,920	392 - 846 2,650	351 - 887 2,670	309 - 928 2,220	268 - 969 2,400	227 - 1011 1,410	186 - 1052 1,160	144 - 1093 n.a.	103 - 1134 n.a.
(9) 0.85	681 - 722 10 <sup>9</sup>	639 - 763 10 <sup>6</sup>	598 - 804 500,000	557 - 846 113,670	516 - 887 45,080	474 - 928 n.a.	433 - 969 n.a.	392 - 1011 n.a.	351 - 1052 n.a.	309 - 1093 n.a.	268 - 1134 n.a.	227 - 1176 n.a.	186 - 1217 n.a.
(10) 0.95	764 - 805 10 <sup>9</sup>	722 - 846 10 <sup>6</sup>	681 - 887 500,000	639 - 928 n.a.	598 - 969 n.a.	557 - 1011 n.a.	516 - 1052 n.a.	474 - 1093 n.a.	433 - 1134 n.a.	392 - 1176 n.a.	351 - 1217 n.a.	309 - 1259 n.a.	269 - 1300 n.a.

Note. 1. Pu = Ultimate Design Load 825 N 2. n.a. = Test results are not available 3. Load range is given in italics, ex., 186 - 557 N for row 5 x column 5.



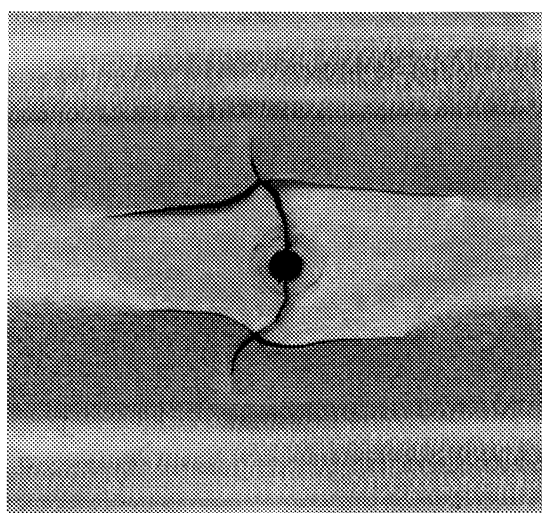
Horizontal Axes are expressed as fractions of the Ultimate Design Wind Load ( $P_U$ ) per Fastener

**Figure 10. Three Dimensional Plot of Cycles to Failure Matrix**

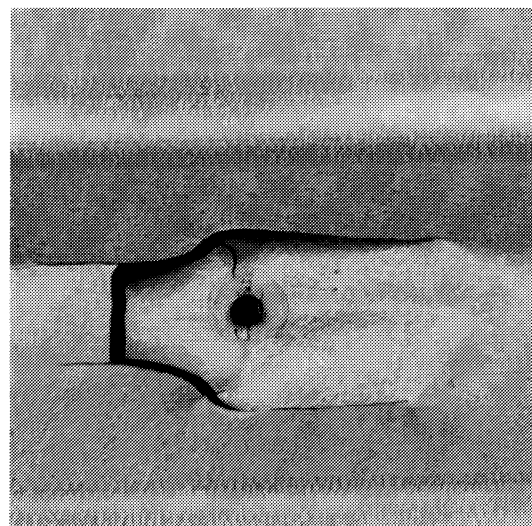
When load was cycled from a nonzero load to a  $P_{max}$  value less than the LPD load, the cracks were identical to those type B or A-B cracks observed in the tests with zero minimum load. In this case it was noted that type B cracks were forming even at a higher maximum cyclic load level of about 500 N. This also confirms the effect of both range and mean level of loading on the fatigue behaviour.

When  $P_{max}$  was greater than the LPD load, crack types observed were not type A as expected, but an H or H\* type (see Figure 11). Cracks always initiated at points away from the fastener hole and propagated in parallel longitudinal directions (parallel to span). Eventually transverse cracks formed at the hole and thus enabled the pull through of fasteners in an H type crack. In the case of H\* type crack, transverse cracks did not form at the hole, but at a point away from the hole and caused tearing. In most cases of H\* type cracking, the specimen was still hanging on a little piece of sheeting as seen in Figure 11 (b), but test was discontinued as it was thought that

damage to roofing was sufficiently severe. As seen in Table 2 (a), both H and H\* type cracks were associated with both smaller and larger  $N_f$ . However, there was little difference in the cracks irrespective of  $N_f$ . In some cases of testing with smaller minimum load, type A cracks were still observed.



(a) Type H



(b) Type H\*

**Figure 11. Additional Typical Cracks Observed on Corrugated Roofing Fastened at Alternate Crests without Cyclone Washers**

As expected, for any mean level of loading, the increase of range of loading decreased the  $N_f$  (see rows of Table 3). The  $N_f$  decreased more rapidly at the beginning than in later stages. However, somewhat an anomalous observation was made when mean level of loading was increased for a fixed value of range as seen from the columns 1 to 5 of Table 3. For example, in the fourth column the  $N_f$  decreased from  $10^9$  to 33,470 cycles during which  $P_{max}$  was increased from 186 to 681 N. When it was increased further to 763 and 846 N,  $N_f$  also increased to 73,590 and 113,670 cycles, respectively. This is because the load cycling occurred predominantly above the LPD load in the latter cases (500 N/f in the second and following cycles), and there was no local plastic buckling deformation after the first cycle in these two tests. In these cases crack type was mainly of type H\*.

Similar trend of greater  $N_f$  for increasing mean level of loading was observed even when it did go through LPD stages (for columns 8 and above). In the ninth column of Table 3,  $N_f$  decreased from 53,900 to 540 cycles when  $P_{max}$  reached the LPD load. Once  $P_{max}$  was greater than the LPD load, increasing the mean level of loading for the same range increased the  $N_f$ , although

cycling still went through the LPD stages. However, it is to be noted that the increase in  $N_f$  was not so significant as in the cases mentioned in the previous paragraph when loading missed the LPD stages. The crack type in these cases was mainly of type H.

In some cases of cycling at lower loads cracks did not initiate from the edge of holes, but at points away from the edge. Eventually the roofing lost an entire piece around the hole, the size of which is slightly smaller than the fastener head. Once a bigger hole formed in this way, cracks initiated from the edge of the bigger hole and propagated in all directions until the fastener pulled through the roofing.

#### 4.2.3 General equation to predict $N_f$ for all loading cases

The fatigue data obtained for roofing (test span = 650 mm) fastened at alternate crests in Sections 4.2.1 and 4.2.2 formed the database from which a general equation to predict  $N_f$  was derived, using a method of multiple variable regression analysis. The variables  $P_{max}$  and range of loading  $R$  were considered the most influential variables to affect  $N_f$ . The effect of the presence of LPD load  $P_b$  was included by expressing  $P_{max}$  and  $R$  as ratios of  $P_b$  which also helped to derive an equation that is dimensionally correct. The value of  $P_b$  was taken as 500 N/f which was the LPD load in the second and following cycles because  $N_f$  will be dependent on this load, rather than on the LPD load in the first cycle. This analysis gave the following equation which provides reasonably good estimates of  $N_f$  for most cyclic load cases.

$$N_f = c \left( \frac{R}{P_b} \right)^{-a} \left( \frac{P_{max}}{P_b} \right)^{-b} \quad (4)$$

where  $c = 10^4$ ,  $a = 3.8$  and  $b = 1.8$

#### 4.2.4 Effect of initially tightened fasteners

Beck (1978) investigated the effect of initially tightened fasteners on the behaviour of corrugated roofing that had a three fasteners per sheet arrangement. His results showed that tighter the fasteners initially, the greater the number of cycles to failure in a fatigue test. He concluded that initial tightening of fasteners had a significant effect on the number of cycles to failure when the maximum cyclic load was below a nominal load of 550 N/f, but this effect was insignificant for greater maximum cyclic loads. In this investigation, only two tests were conducted on roofing fastened with initially tightened screws at alternate crests. The first test was a fatigue test on a test span of 650 mm with load cycling from zero to 600 N/f, but the second was a static test to failure on a test span of 500 mm. Both central fasteners at the central support in the fatigue test had the special arrangement described earlier in Section 3.4 for measuring the tensile load in each fastener.



The specimen was statically loaded to 600 N/f several times before the fatigue test in order to establish the actual variation of load in the fasteners with applied uplift load. The central fasteners at the critical central support were tightened until the reading for each load cell attached to the fastener (see Figure 5) indicated 200 N, but other fasteners were tightened such that they had the same crest setting as the central fasteners at the central support, i.e., about 5 mm difference in height between the screwed and unscrewed crests. Tightening of fasteners at the crests would have created a reaction between the adjacent valleys and the batten. This reaction force was not measured, but was anticipated to be equal to 200 N, the initial force in the fastener.

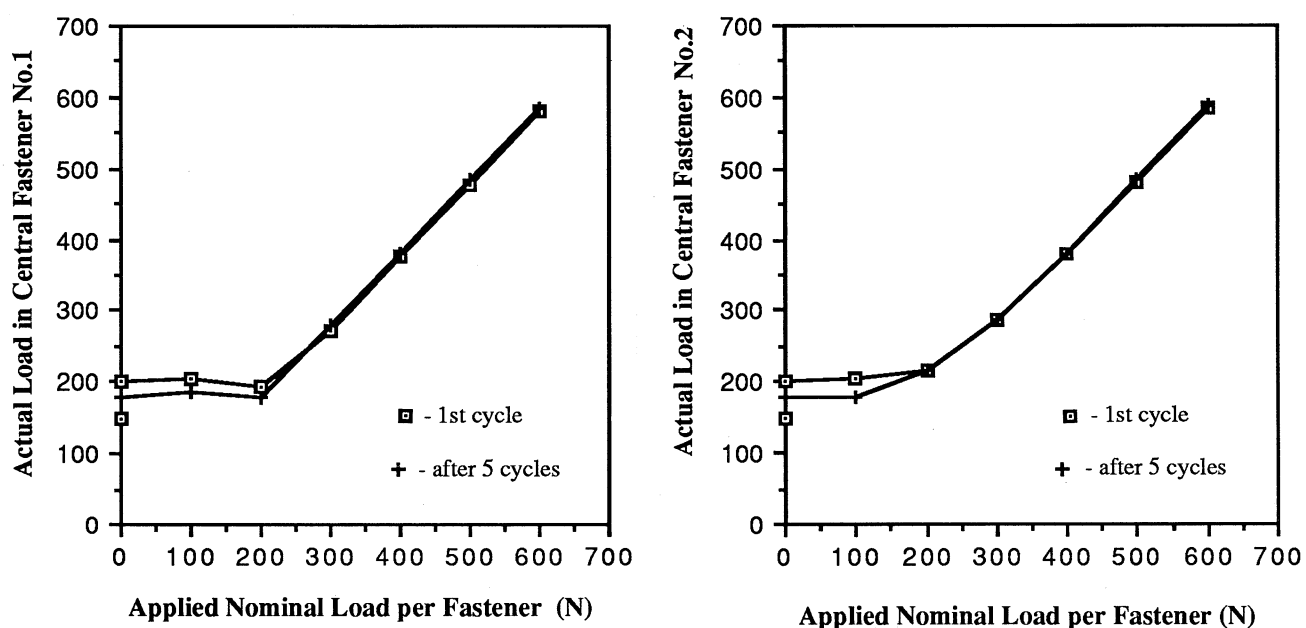


**Figure 12. Variation of Load in Fasteners**

Figure 12 shows the variation of load in the central fasteners at the central support when the specimen was loaded in uplift and unloaded. In this figure the horizontal axis is the nominal load in each central fastener at the central support due to the applied loading if there was no initial tightening. This load was obtained from the load cell above the portal frame that provided the total reaction at the central support. The applied uplift load at midspans had to first lift the valleys off the batten, and only after which the tensile force in the fasteners increased. This is indicated by the initial plateau followed by the steeply rising curve in Figure 12. Beck (1978) also observed a similar variation in load per fastener in his investigation. It is to be noted that a steady increase in the fastener was observed beyond 200 N/f of applied uplift loading. Finally when the applied nominal load per fastener reached 600 N, the actual load in the central fasteners were 580 and 585 N. This meant that the edge fasteners at the central support would have had a force of 618 N on average.

Ideally one would expect 600 N in each central fastener as there would be no reaction at the valleys beyond the flat part of the curve. However, this deviation of only 3.5% is considered quite satisfactory, and thus reaffirms the relatively uniform load distribution among the fasteners across the width of roofing in the test set-up used in this investigation.

When the specimen was unloaded, the load in each central fastener returned to 150 N. The fasteners were re-tightened to 200 N and the specimen loaded again. Eventually the loading range in the central fasteners stabilised at 180 N to 585 N and 590 N (see Figure 12). It is to be noted that the corresponding applied nominal load per fastener ranged from zero to 600 N. Thus it could be said that the effect of initial tightening of fasteners is to reduce the range of loading in each fastener by approximately the initial tightening force, which in turn would cause greater cycles to failure in a fatigue test. This was indeed the case when the same specimen was cyclically loaded from zero to 600 N. It lasted 2450 cycles compared to 1560 cycles when a similar specimen was tested without any initial tightening (see Table 1 (c)). One of the edge screws pulled through first thus confirming the observation regarding slightly greater load in edge screws during preliminary static tests.

During the fatigue test the minimum cyclic load in each fastener decreased (from 180 N) with increasing number of cycles as the area around the holes began to distress and dimple. Thus the range of loading in each fastener increased gradually that would have decreased the cycles to failure. Even then there was about 80% increase in the cycles to failure in this case. Similar increase in cycles to failure is anticipated for other loadings up to the LPD load of 650 N/f. However, similar improvement cannot be expected for maximum cyclic load greater than the LPD load as load cycling in this case will go through local plastic buckling stages.

Figure 13 presents the results of the second test, the static test for which the fasteners were initially tightened to about 5 mm difference in height between adjacent crests. Although loads in individual fasteners at the central support were not measured, it is anticipated that the nominal initial fastener load would have been 200 N. The upward deflections of the crests in the present test were measured from the initially deformed position. Results from this test are compared with those from a test reported earlier (Mahendran, 1988b) in which the specimen was not tightened initially. As seen from the figure the unscrewed crests did not deflect significantly more than the screwed crests during loading when the specimen was initially tightened. Initial tightening had negligible effect on the LPD load and the ultimate static failure load. This is not surprising as at a nominal fastener load of greater than 200 N, valleys would have separated from the battens below and after which the fastener load was dependent only on the applied uplift load on the roofing.

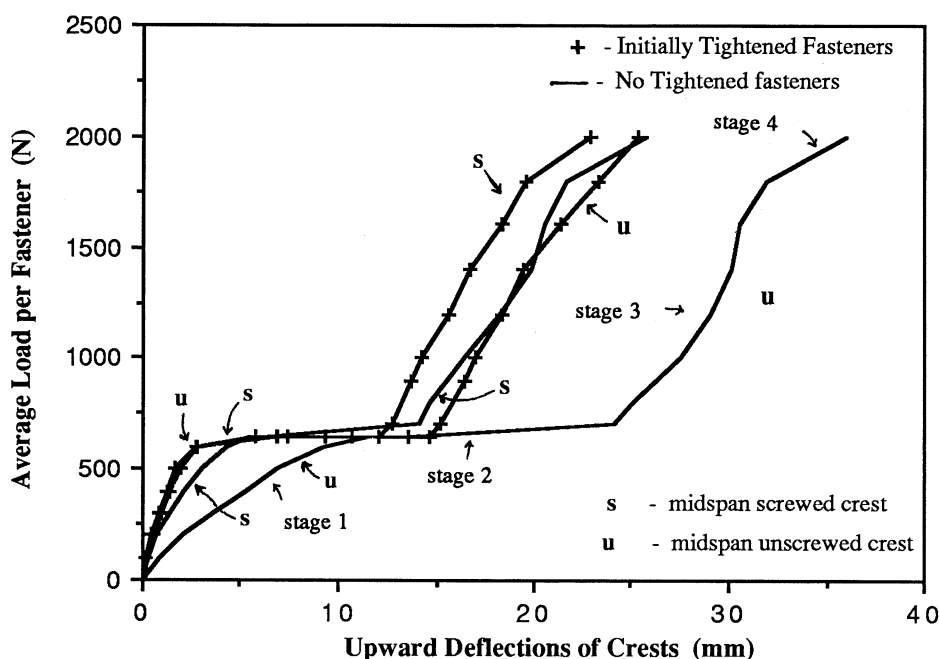


**Figure 13. Load-deflection Curves for Corrugated Roofing with Initially Tightened Fasteners at Alternate Crests**

#### 4.2.5 Effect of loading frequency

The loading frequency during a laboratory test should be commensurate with that occurring in actual prototype conditions (Mann, 1974). It is believed that roof claddings are subjected to fluctuating wind loading at a frequency between 1 and 3 Hz during tropical cyclones. This is in agreement with the observations during cyclone Tracy when an engineer-owner of a Darwin house noticed the roof of his house to vibrate at a frequency of approximately 2 Hz (Beck and Morgan, 1975), and also with the actual measurements on a full scale house in England which revealed that the maximum power spectra of the roof pressure occurred at a frequency of 1.5 Hz (Eaton and Mayne, 1974). In the past, laboratory tests simulating cyclonic wind loading have been conducted at frequencies in the range of 0.1 to 2.0 Hz. Selection of a particular frequency has been mainly dependent on the capability of the testing machine to apply a certain range of loading.

TR440 (EBS, 1978) imposes a maximum limit of 3 Hz on the loading frequency for tests on roof claddings, but not a minimum limit (clause 2.4 (f)). Therefore a performance test at a very low frequency of 0.01 Hz (say) is permissible under the current recommendations of TR440 although the effect of such low frequency on the results is not known. Hence at the recent workshop on the review of TR440, it was decided that effects of frequency on fatigue test results of roof claddings be investigated.

According to D'Isa (1968), metal fatigue has always been considered to be insensitive to the commonly used loading frequencies in the range of 1.5 to 150 Hz. At very high frequencies greater than 150 Hz the fatigue strength of most metals increases, but there is evidence that for steels there occurs a decrease again above a frequency of 1500 Hz. At lower frequencies, there is a tendency toward lower fatigue strength possibly because more time is available for plastic flow in the crystals. Hence it may be said that TR440 recommendations are conservative as it does not restrict lower frequency tests.

There is no need to do tests on roof claddings at a frequency greater than 3 Hz as these tests involve a low cycle fatigue problem. Even the modern testing machines cannot cope with flexible light gauge metal roof claddings satisfactorily at higher frequencies. The main question in the past has been on how slow can a test be done. This investigation attempted to resolve this by means of a limited number of tests on corrugated steel roofing and the results are presented in Table 4. In most cases there was a slight reduction in the number of cycles to failure  $N_f$  for lower frequency, but the reduction was insignificant to conclude that testing at lower frequencies will cause premature fatigue failure. In fact, in one test  $N_f$  increased with lower frequency. Therefore it is considered that clause 2.4 (f) and the associated commentary of TR440 on loading frequency may be revised to include the following.

"Loading frequency for Type II test should be in the range of 1.0 to 3.0 Hz in order to simulate the actual loading frequency due to cyclones. However, a lower loading frequency up to 0.01 Hz may be used if the testing equipment has a limitation in loading at higher frequencies. The effect of such lower frequency tests on the results is in general conservative and can be considered insignificant".

Although no test was done relating to Type I test for wall structures, it is considered that similar changes can be made to the current clause which restricts only the maximum loading frequency to 0.3 Hz.

**Table 4 Effect of Loading Frequency**

Tests on Corrugated Roofing Fastened at Alternate Crests without Cyclone Washers

Test Span (mm)	1000			650
Cyclic Load Range (N/f)	0 - 350	0 - 400	0 - 450	0 - 550
$N_f$ at a Frequency of 1.5 Hz	39,700	9,040	1,950	-
1.0 Hz	-	-	-	2,250
0.3 Hz	-	7,200	-	-
0.1 Hz	36,570	-	1,590	-
0.03 Hz	-	-	-	2,360

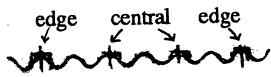
### 4.3 Roofing Fastened at Alternate Crests with Cyclone Washers

Based on a finite element analysis and a limited number of fatigue tests, it was concluded that the use of cyclone washers in fastening the corrugated roofing at alternate crests is an effective method to prevent the premature cracking under the fastener heads and the resulting disengagement of roofing (Mahendran, 1988a,b). Since then more fatigue tests have been conducted on a common span (test span of 650 mm) and the results are presented in this section (Table 5). It is to be noted that in this section cyclone washers are simply referred to as washers.

Preliminary static tests on roofing of 650 mm test span during which each specimen was loaded up to the maximum cyclic load revealed the occurrence of local plastic buckling in the vicinity of central support fasteners at a load level between 900 and 950 N/f. This is in agreement with previously reported test result of 900 N/f (Mahendran, 1988b). Due to the presence of local plastic buckling, fatigue cracking was mainly of two types depending on whether the maximum cyclic load  $P_{max}$  was above or below the LPD load. When the results for the case of zero minimum load without any overloading prior to cyclic loading (Nos. 1 to 7 in Table 5) are plotted, a fatigue curve similar to Figure 6 in Section 4.2.1 with different segments is obtained (Figure 14). Both  $P_{max}$  and  $N_f$  are plotted on a log scale in order to obtain a linear relationship that describes best the test data. However, even when only  $N_f$  is plotted on a log scale, test data appeared to fall on straight lines reasonably well as in the case of roofing without washers, but this fatigue curve is not presented here. In order to study the relative increase in  $N_f$  when washers are used, the fatigue curve for the case of roofing without washers is also plotted in Figure 14.

**Table 5      Fatigue Test Results of Corrugated Roofing  
Fastened at Alternate Crests with Cyclone Washers**

(Test span = 650 mm except in No.10 for which it is 1000 mm)



Cyclic Load Range (N/f)	Number of Cycles to		Type of Crack	Pull Through at
	Crack Initiation $N_i$	Failure $N_f$		
(1) 0 - 600	70,000	245,360	CW-B	Edge Hole
(2) 0 - 700	n.o.	65,170	CW-B	Central Hole
(3) 0 - 800	n.o.	11,300	CW-B	Edge Hole
(4) 0 - 900	150	2,340	CW-AB	Central Hole
(5) 0 - 950	100	1,950	CW-A	Central Hole
(6) 0 - 1100	80	860	CW-A	Central Hole
(7) 0 - 1200	50	540	CW-A	Central Hole
(8) Overload to 950 then 0 - 700	50	9,030	CW-A*	Central Hole
(9) Overload to 950 then 0 - 600	50	23,310	CW-A*	Edge Hole
(10) 0 - 550	28,000	n.a.	n.a.	n.a.

Note 1. n.o. - Crack initiation was not observed in this test

2. n.a. - Test discontinued when longitudinal cracks appeared under the washer edges.  
If continued, it would have led to a CW-B type of cracking and failure.

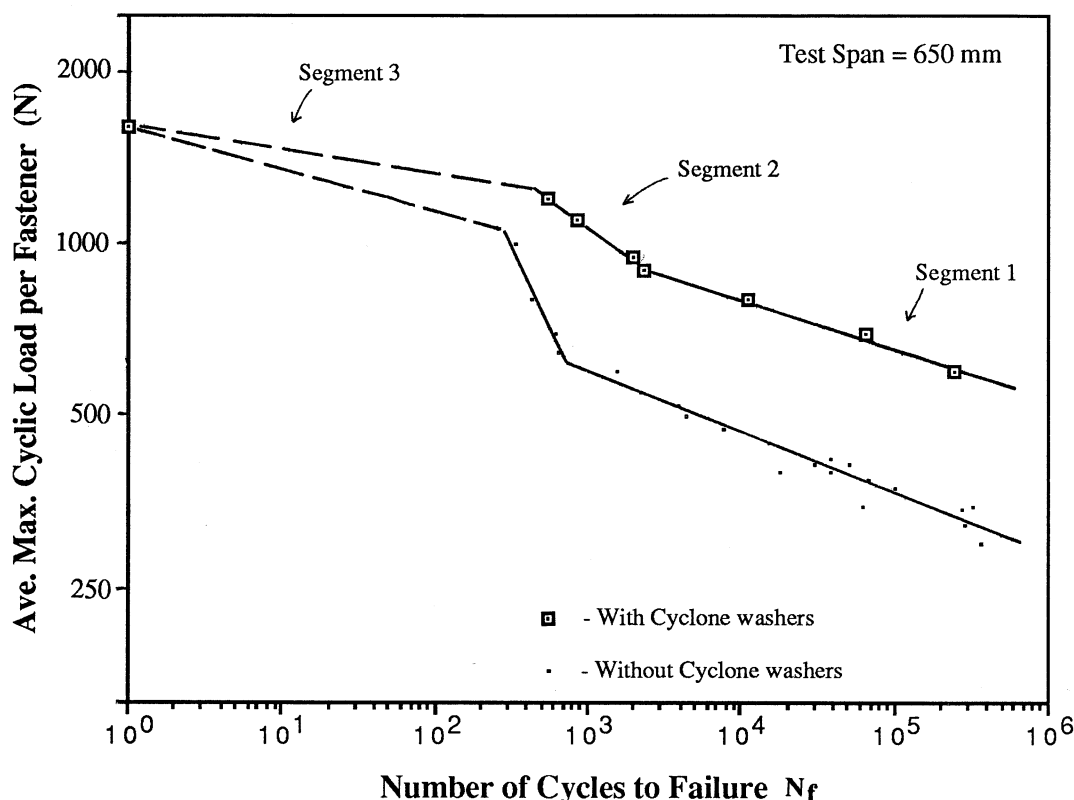
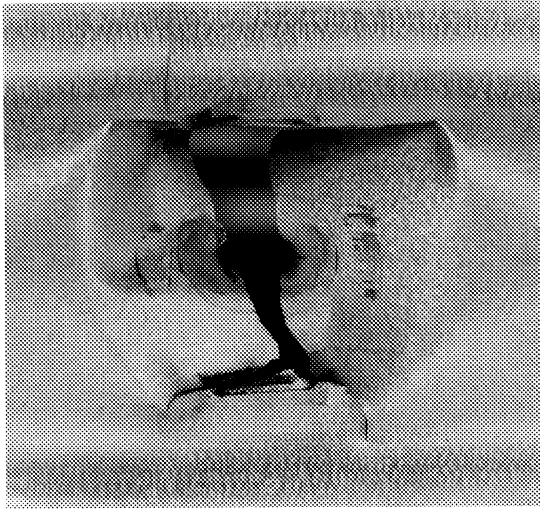


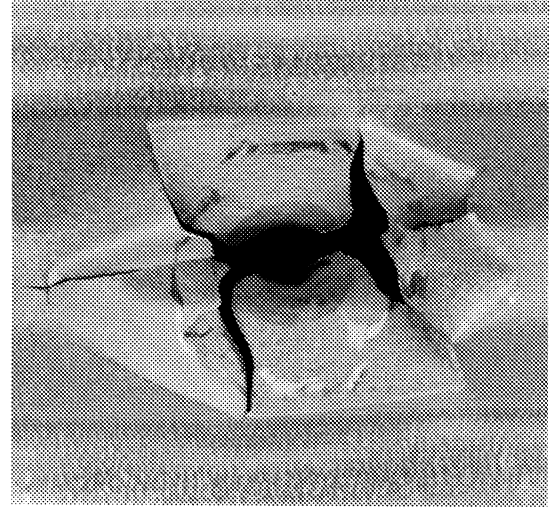
**Figure 14. Fatigue Curve for Corrugated Roofing Fastened at Alternate Crests with Cyclone Washers** (Cycling from zero minimum load)

The first segment of the fatigue curve corresponds to the case when  $P_{max}$  is less than the LPD load of 900 N/f. As  $P_{max}$  was decreased  $N_f$  increased rapidly. The significant improvement when washers were used is to be noted, for example,  $N_f$  increased from 1,560 to 245,360 cycles for the same maximum cyclic load of 600 N/f which means an increase in the life of roofing by 15,630%. Similar improvements are observed at all other loads up to the LPD load.

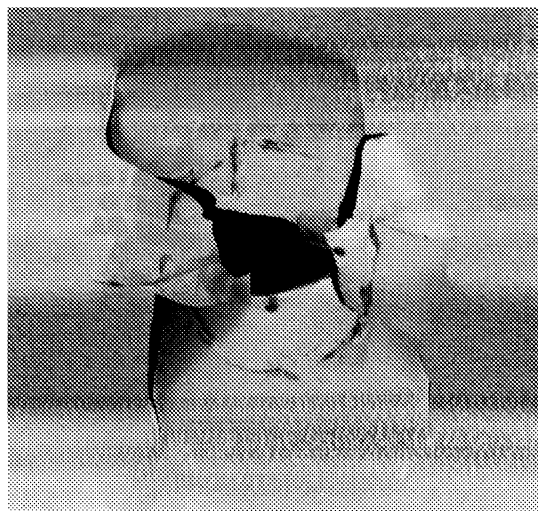
In the case of first segment, cracks always appeared first under the edges of cyclone washers in the longitudinal direction. The finite element analysis of roofing carried out earlier (Mahendran, 1988b) predicted high stresses under the edge of washers, rather than around the edge of fastener holes, and thus confirm the above observation regarding the first location of cracking. These longitudinal cracks extended to more than 50 mm (i.e., beyond the length of washer) in most cases as load cycling progressed. Eventually transverse cracks formed and developed to an extent that let the entire fastener-washer assembly to pull through the roofing. Figure 15 (a) shows a typical crack type (CW-B) in this case. Examination of washers during and after testing showed that washers suffered no damage due to load cycling (i.e., no bending or flattening of washers).



(a) Type CW-B



(b) Type CW-A



(c) Type CW-A\*

**Figure 15. Typical Cracks Observed on Corrugated Roofing  
Fastened at Alternate Crests with Cyclone Washers**

The second segment of the fatigue curve corresponds to the case when  $P_{\max}$  is greater than the LPD load of 900 N/f. This segment involves cycling at very high stresses and thus smaller  $N_f$ . The fatigue performance deteriorated rapidly as  $P_{\max}$  was increased above the LPD load. This rapid deterioration was not only because that load cycling had to go through local plastic buckling stages, but also because the thin washers became ineffective soon after the first cycle of loading. The 1 mm thick washers were bent and flattened severely as seen in Figure 16. In the second and following cycles of loading it was found that local plastic buckling occurred at a lower load of 550 N/f (approximately), and not at 900 N/f as in the first cycle of loading. Although this is somewhat similar to the observation where the LPD load decreased from 650 N/f to 550 N/f in the case of alternate crest fastening without washers (see Section 4.2.1), the deterioration in this case was severe. Hence the fatigue behaviour of corrugated roofing fastened with washers was not much better than that of roofing fastened without washers once the maximum cyclic load was greater than the LPD load.

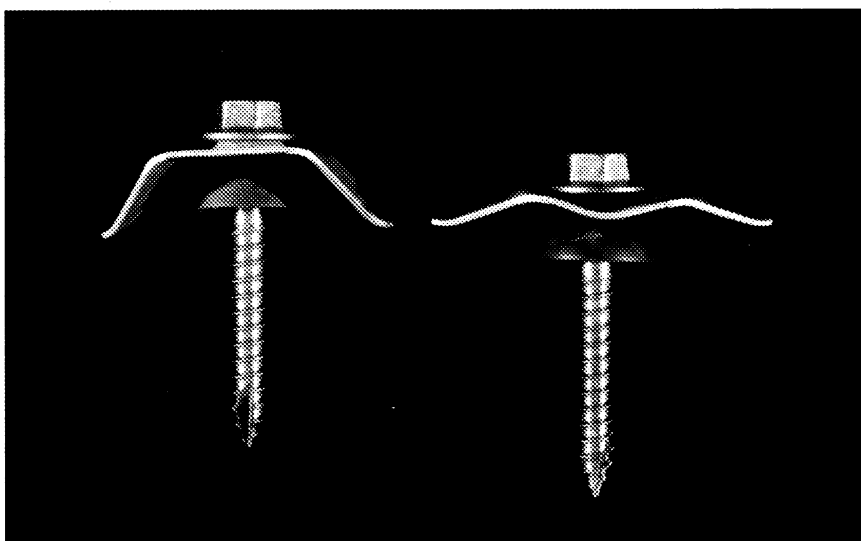


**Figure 16. Damaged Cyclone Washers**

In the second segment cracks initiated from the edge of the hole within the first 100 cycles and propagated rapidly in all directions. When the cracks had extended sufficiently long (more than 50 mm), the entire fastener-washer assembly pulled through the roofing. Figure 15 (b) shows a typical crack type in this case (CW-A).

During the transition from Segment 1 to Segment 2 at a load of 900 N/f, a crack type somewhat between CW-A and CW-B was observed and is referred to as CW-AB in Table 5.

During the third segment shown in Figure 14, fatigue cracks formed during initial cycles as in the case of Segment 2, but roofing failed by buckling and yielding at midspans (static failure mode) before a fatigue failure could occur. Hence the third segment should not be considered as part of



the fatigue curve and thus is shown by a dashed line in Figure 14. Similar observation was made earlier in the case of roofing fastened at alternate crests without cyclone washers.

For Segments 1 and 2 of the fatigue curve shown in Figure 14, mathematical equations relating  $P_{max}$  and  $N_f$  were derived as it was done in the case of roofing fastened at alternate crests without washers. These equations are given below.

$$N_f = c \cdot P_{max}^{-b} \quad (5)$$

where

$c = 10^{38}$	and	$b = 11.71$	for Segment 1 and
$c = 10^{18.9}$	and	$b = 5.25$	for Segment 2.

Two tests were conducted to study the effect of overloading once before cyclic loading (see Table 5). In the first test the specimen was first loaded up to 950 N/f and unloaded. This static overloading caused local plastic buckling at the central support fasteners and produced bent and flattened washers similar to that shown in Figure 16. Following this, the specimen was cyclically loaded from zero to 700 N/f until failure. The specimen failed very prematurely after only 9,030 cycles compared to 65,170 cycles when there was no prior overloading. Thus an initial overloading by only 35% had caused a huge reduction in roofing's life span. The reason for this behaviour can be attributed to the reduced local plastic buckling load and the ineffectiveness of the flattened washers after the overloading. The reduced LPD load was 550 N/f as mentioned earlier in the case of Segment 2, and thus cycling with a maximum cyclic load of 700 N/f would have gone through the LPD stages (at 550 N/f). In the second test with prior overloading the specimen was cyclically loaded from zero to 600 N/f after an overloading by 58% to 950 N/f. In this case  $N_f$  was reduced from 245,360 to 23,310 cycles.

In the two tests with prior overload, cracks initiated from the edge of hole and propagated in all directions until the cyclone washer-fastener assembly pulled through the roofing. Crack type in this case, referred to as CW-A\* in Table 5, was somewhat similar to CW-A observed in Segment 2, and is shown in Figure 15 (c). As seen in Figures 15 (a) to (c), for all the cases of loading, roofing had cracked and torn very severely by the time the washer-fastener assembly pulled through the roofing. In most tests only one cyclone washer-fastener assembly pulled through the roofing, but most other holes at the central support had also cracked very severely at failure.

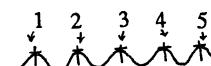
Fatigue tests were conducted only on one test span (650 mm). However, during the static tests on roofing of different spans (1000, 650, 500 and 250 mm) fastened at alternate crests with cyclone washers, the LPD load increased from 750 to 1300 N/f as the span was reduced. This research programme has shown that the fatigue behaviour of corrugated roofing is very much dependent on the LPD load. Hence these results from static tests indicate that shorter spans of roofing will perform better in fatigue than longer spans of roofing at the same load per fastener, and thus lead to the conclusion that both loading parameters, load per fastener and the bending

moment at central support are critical in controlling the fatigue behaviour of roofing fastened with washers.

#### 4.4 Roofing Fastened at Every Crest without Cyclone Washers

During all the fatigue tests, load was cycled from zero minimum load to various preset maximum loads at a constant frequency of 1.5 Hz. Tests were conducted on three test spans of 250 mm (short span), 500 mm (medium span) and 1000 mm (long span). Table 6 and Figure 17 present these fatigue test results.

**Table 6**      **Fatigue Test Results of Corrugated Roofing**  
Fastened at Every Crest without Cyclone washers



(a) Test Span = 250 mm (short span)

Cyclic Load Range (N/f)	Number of Cycles to		Type of Crack	Pull Through at
	Crack Initiation $N_i$	Failure $N_f$		
(1) 0 - 600	n.o.	78,890	EC-B	3rd, 4th & 5th Holes
(2) 0 - 600	n.o.	34,200	EC-B	Edge Hole
(3) 0 - 650	14,400	52,770	EC-B	1st, 2nd & 3rd Holes
(4) 0 - 700	1,100	2,340	EC-A	1st & 2nd Holes
(5) 0 - 700	500	2,800	EC-A	3rd & 4th Holes
(6) 0 - 800	500	800	EC-A	All Central Holes

(b) Test Span = 500 mm (medium span)

Cyclic Load Range (N/f)	Number of Cycles to		Type of Crack	Pull Through at
	Crack Initiation $N_i$	Failure $N_f$		
(1) 0 - 450	25,000	42,180	EC-B	2nd & 3rd Holes
(2) 0 - 500	n.o.	15,320	EC-B	3rd & 4th Holes
(3) 0 - 500	n.o.	10,120	EC-B	2nd Hole
(4) 0 - 550	1,800	10,040	EC-B	1st & 2nd Holes
(5) 0 - 600	1,200	2,070	EC-A	4th Hole
(6) 0 - 650	640	1,190	EC-A	2nd & 3rd Holes

(c) Test Span = 1000 mm (long span)

Cyclic Load Range (N/f)	Number of Cycles to		Type of Crack	Pull Through at
	Crack Initiation $N_i$	Failure $N_f$		
(1) 0 - 300	n.o.	50,970	EC-B	1st & 2nd Holes
(2) 0 - 325	14,000	41,860	EC-B	All Central Holes
(3) 0 - 350	2,500	7,500	EC-A	3rd, 4th & 5th Holes
(4) 0 - 375	2,600	4,280	EC-A	Edge Hole

Note 1. n.o. - Crack initiation was not observed in this test.

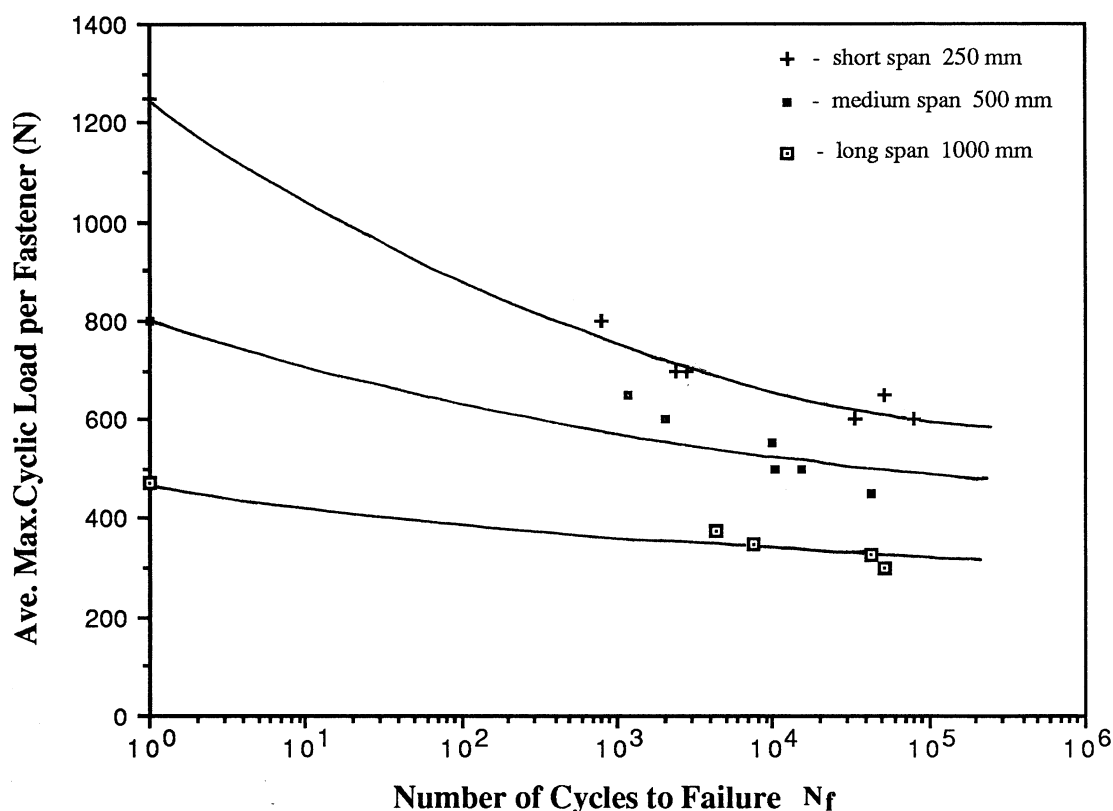
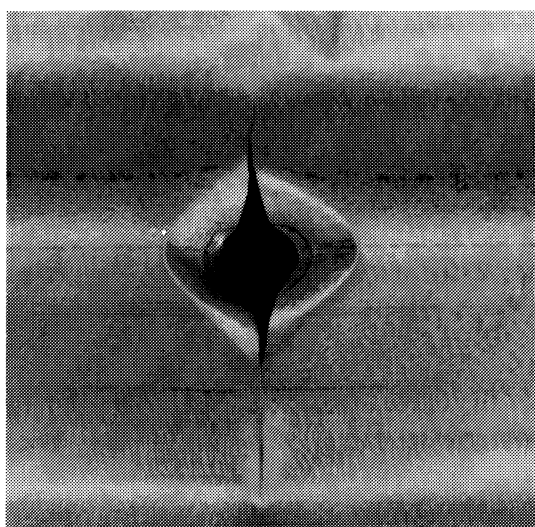


**Figure 17. Fatigue Curves for Corrugated Roofing Fastened at Every Crest without Cyclone Washers (Cycling from zero minimum load)**

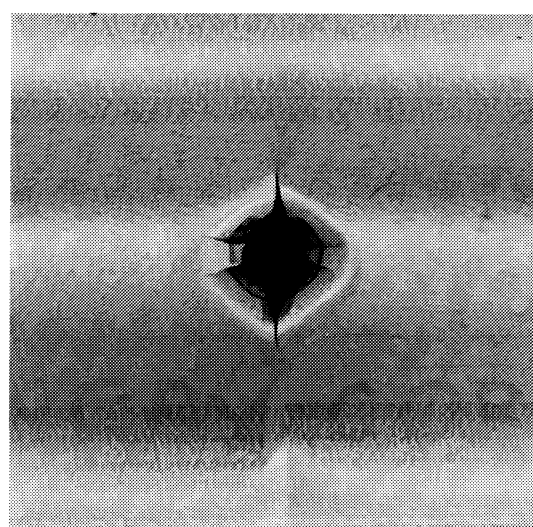
Fatigue test results correlate quite well with the static results reported earlier (Mahendran, 1988b). Unlike the fatigue curves obtained for roofing fastened at alternate crests, the fatigue curves in this case were smooth continuous curves and clearly indicated that shorter spans of roofing have a greater  $N_f$  than longer spans of roofing for the same maximum cyclic load per fastener. This is to be expected as no anomalous observation was made in the static investigation of roofing fastened at every crest. During static tests, roofing behaved almost like an ideal two-span continuous beam and its behaviour was predictable even by simple engineering calculations. Hence in this case both load per fastener and bending moment at the central support govern the fatigue behaviour.

In the static investigation, very little cross-sectional distortion and thus no premature local plastic buckling was observed for all the spans. Diamond-shaped dimples appeared under the central fastener heads only at a higher load closer to the ultimate static failure load for each span. Hence as anticipated the fatigue behaviour of roofing in this case is significantly better than that in the case of alternate crest fastening. Except for the long span roofing, a greater design load per fastener can be used when every crest is fastened. This means that more than twice the uplift pressure can be applied if every crest is fastened rather than alternate crests are fastened.

The static analytical investigation using a finite element analysis showed that there are larger stresses in the vicinity of central support fastener holes than anywhere else in the roofing. Thus cracks always appeared at the edge of the central support fastener holes. These cracks propagated mainly in the transverse direction (perpendicular to span) until the fastener pulled through. Figure 18 shows the crack types observed in this case. There were two types of cracks (referred to as EC-A and EC-B in Table 6) depending on the cyclic load levels for each span. However, there was no significant difference between the two cracks in this case as in the case of type A and B cracks with alternate crest fastening. This was essentially because the local plastic buckling deformations that caused such a difference in the latter was absent in this case of every crest fastening. Despite this there was a sudden change in  $N_f$  when crack type changed from one to another as seen in Table 6.



(a) Type EC-A



(b) Type EC-B

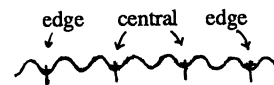
**Figure 18. Typical Cracks Observed on Corrugated Roofing  
Fastened at Every Crest without Cyclone Washers**

#### **4.5 Roofing Fastened at Alternate Valleys**

A static analysis of corrugated roofing showed that local plastic buckling did not occur when roofing was fastened at alternate valleys (Mahendran, 1988b). Thus the stresses in the vicinity of the fastener holes are not as large as those in the case of alternate crest fastening at nominally the same load per fastener. Hence it is anticipated that fatigue performance will be improved when fastened at alternate valleys rather than at alternate crests. A total of nine cyclic tests with

zero minimum load were conducted on roofing of test span of 650 mm fastened at alternate valleys at a frequency of 1.0 Hz. Results are presented in Table 7 and as a fatigue curve in Figure 19.

**Table 7 Fatigue Test Results of Corrugated Roofing**  
Fastened at Alternate Valleys - Test span = 650 mm



	Cyclic Load Range (N/f)	Number of Cycles to		Type of Crack	Pull Through at
		Crack Initiation $N_i$	Failure $N_f$		
(1)	0 - 400	300,000	405,130	VB	Central Hole
(2)	0 - 500	65,000	105,550	VB	Central Hole
(3)	0 - 600	34,000	49,500	VB	Edge Hole
(4)	0 - 700	15,000	20,690	VB	Edge Hole
(5)	0 - 800	n.o.	20,170	VB	Edge Hole
(6)	0 - 900	n.o.	3,700	VA	Central Hole
(7)	0 - 1000	n.o.	1,930	VA	Central Hole
(8)	0 - 1200	n.o.	10,020	VA	Central Hole
(9)	0 - 1400	n.o.	3,260	VA	Edge Hole

Note 1. n.o. - Crack initiation was not observed in this test.

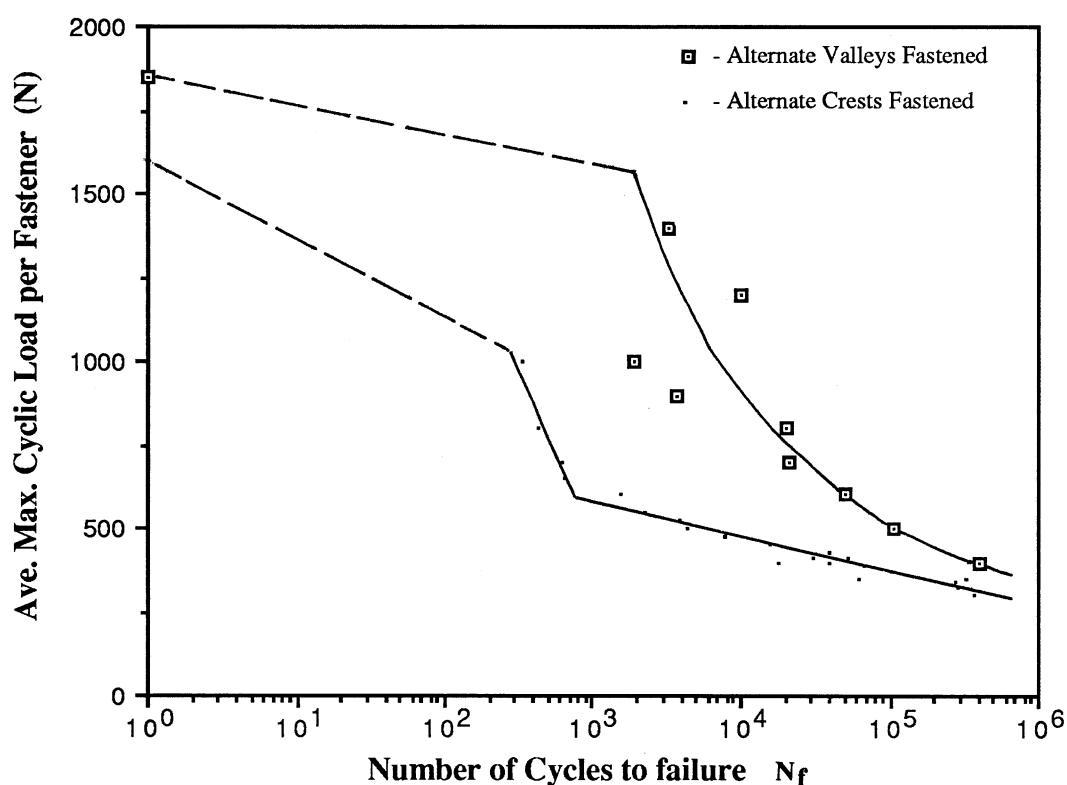


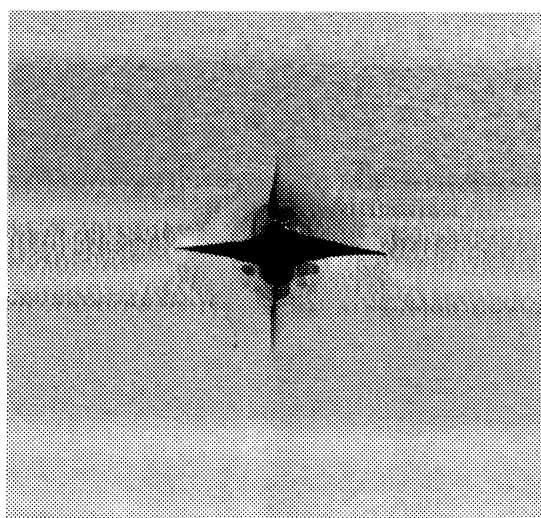
**Figure 19. Fatigue Curve for Corrugated Roofing Fastened at Alternate Valleys**  
(Cycling from zero minimum load)

Comparison of these results with those in the case of alternate crest fastening in Figure 19 clearly shows the improvement in fatigue performance when alternate valleys are fastened. For example,  $N_f$  increased from a mere 1560 cycles to 49,500 cycles for a nominal cyclic load range of 0 to 600 N/f. Despite this better fatigue performance, it is difficult to change the current Australian building practice of fastening at alternate crests as it is believed that leakage cannot be prevented if valleys are fastened. If the leakage problem can be overcome and alternate valley fastening is adopted, the design load per fastener can be increased by at least 50%.

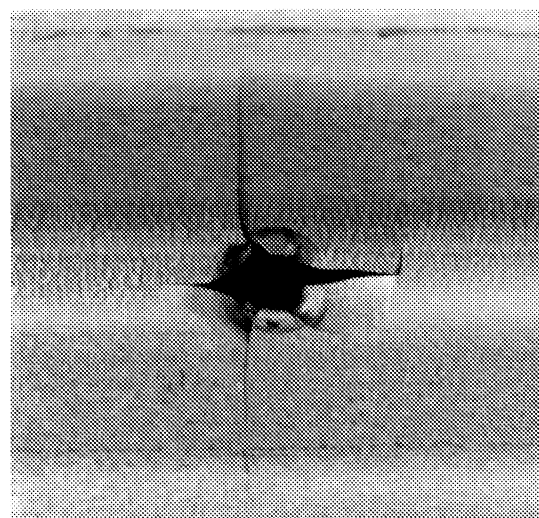
When roofing fastened at alternate valleys was subjected to increasing static uplift load, it became stiffer before it failed at midspans (Mahendran, 1988b). Accordingly, as the maximum cyclic load was increased the  $N_f$  value did not decrease so much, as is seen from the steeper part of the fatigue curve in the range of 800 to 1400 N/f.

The dashed line in the case of alternate valley fastening in Figure 19 belongs to a static mode of failure and as such does not belong to the fatigue curve. In this segment the roofing buckled and yielded at midspans before a fatigue failure could occur at the central support fastener holes.

Cracks always initiated from the edge of central support fastener holes, in most cases in the transverse direction, and propagated in both longitudinal and transverse directions until one or more fasteners pulled through the roofing. Typical cracks that formed in this case are shown in Figure 20. Crack type VB was observed for lower loads (larger  $N_f$ ) whereas crack type VA was observed for higher loads (smaller  $N_f$ ).



(a) Type VA



(b) Type VB

**Figure 20. Typical Cracks Observed on Corrugated Roofing Fastened at Alternate Valleys**

Fatigue tests were conducted for only one test span (650 mm). Without the fatigue test results on other spans, a question of which loading parameter controls the fatigue behaviour cannot be answered. However, static results are available for many test spans of 250, 500 and 650 mm. Shorter spans had relatively greater stiffening under increasing uplift loads, leading to significantly greater ultimate failure load per fastener. Further, when alternate valleys were fastened, there was no such local plastic buckling occurring at the same load per fastener for all the spans as in alternate crest fastening. Therefore it is anticipated that both loading parameters, the load per fastener and the bending moment at central support, are critical parameters in the fatigue behaviour of roofing fastened at alternate valleys.

## 5. IMPLICATIONS OF THE RESULTS OBTAINED

In this section all the results presented and discussed individually in the previous sections are considered together in discussions relating to specific topics.

### 5.1 Comparison of Fatigue Performance of Roofing with Different Fastening Systems

Due to the absence of premature local plastic buckling deformations, the fatigue performance of roofing with fastening systems other than alternate crest fastening appears to be superior to that of roofing fastened in the usual way at alternate crests. From the fatigue curves obtained in this investigation the cyclic load range corresponding to an  $N_f$  of 10,000 cycles is determined for each of the fastening system. A comparison of these loads in Table 8 clearly indicates the superiority of one fastening system over the other with regard to fatigue performance.

**Table 8. Comparison of Fatigue Performance**

Test Span (mm)	Fastening System	Cyclic Load Range (N) for an $N_f$ of 10,000 cycles
(1) 650	Alt. Crest Fastening without cyclone washers	0 - 470
(2) 650	Alt. Crest Fastening with cyclone washers	0 - 800
(3) 650	Alt. Valley Fastening	0 - 850
(4) 500	Every Crest Fastening without cyclone washers	0 - 500

Although alternate valley fastening and every crest fastening appear to be superior in fatigue performance, they are not acceptable to the building industry unless the problems associated with them are overcome. The manufacturers of corrugated roofing recommend only alternate crest

fastening with and without cyclone washers for cyclone prone areas. Alternate valley fastening is not recommended for roof claddings due to the possibility of water leakage, particularly if it were to be used in the cyclone prone areas which have a long wet season. Therefore unless a water-proof fastener assembly is developed, alternate valley fastening cannot be advocated despite its superior fatigue performance. Similarly in the case of every crest fastening, there lies a problem of splitting timber battens/purlins as they will be screwed at a closer spacing of 76 mm. Therefore every crest fastening also cannot be recommended for corrugated roof claddings.

The use of cyclone washers at alternate crests is found to improve the fatigue performance by delaying the local plastic buckling deformation significantly (greater LPD load). However, except in N.T., these washers are not commonly used by the builders. According to one of the leading manufacturers of roofing fasteners, the number of No.14 x 50 mm fasteners with cyclone washers sold during the last three months was only 25% of the number of such fasteners sold without cyclone washers. One of the leading manufacturers of corrugated roofing was also in agreement with the above comments. It is believed that the unpopularity of these washers is due to the difficulty in installing them as the metal washer tends to rotate during fastening. This means that the builder has to use one hand to hold the washer in position and the other to hold the drill during installation which results in increased labour cost. Cyclone washer-fastener assemblies are twice as expensive as the normal fasteners. But by using these washers greater spans can be used which should reduce building costs. Hence the net increase in building cost (if any) can never be greater than a very small percentage of the overall building cost. It is to be noted that despite this, builders prefer not to use cyclone washers as it is permitted by the current building regulations. Thus alternate crest fastening without cyclone washers still remains the most commonly used fastening system in the cyclone prone areas.

## **5.2 Current Design Loads in Relation to LPD Load**

### **5.2.1 Alternate crest fastening without cyclone washers**

When roofing was fastened at alternate crests without cyclone washers, the low cycle fatigue cracking that occurred prematurely could be considered to be due to the local plastic buckling behaviour at comparatively smaller loads and as such the LPD load is an important parameter governing the fatigue behaviour of roofing. Based on an earlier static investigation and some preliminary static test results in this investigation, the LPD load can be assumed to be 600 N/f for all the common spans. As anticipated from the static tests and confirmed by fatigue tests, the fatigue resistance is reduced by an order of magnitude when the applied load is greater than the LPD load. Hence the LPD load should be considered the ultimate load from a fatigue strength consideration although the corresponding ultimate static load is many times greater than the LPD load. However, it is interesting to note that the current design load used by the manufacturer of



corrugated roofing is 550 N/f (LBI, 1987) which was determined based on results from TR440 tests (EBS, 1978). Although all the tests in this investigation indicated very little variation in the LPD load, the lower bound of the LPD load in a realistic situation could be less than that observed during these laboratory tests. This means that the current design load may be too close to the LPD load

During rapidly fluctuating and largely unknown cyclonic wind forces, the occurrence of at least a few cycles in excess of design load will cause local plastic buckling under the fastener heads for such a relatively high design load adopted at present for roofing fastened at alternate crests without cyclone washers. In fact such loading above the design load can cause a severe reduction in the fatigue life of roofing as it was found from a limited number of tests. A specimen (test span = 650 mm) that was preloaded by a few cycles (6) of loading above the LPD load (zero to 700 N/f) failed after only 21,000 cycles at a lower load level of zero to 350 N/f. However, it was expected to have survived about 150,000 cycles if it had not been overloaded at the beginning. In another test, an identical specimen was first subjected to a few cycles of zero to 600 N/f loading which did not cause local plastic buckling deformations at the fastener holes, but would have caused yielding at some locations around the fastener holes. This specimen survived about 87,000 cycles of zero to 350 N/f loading. These results indicate that load cycling at lower levels can also cause severe fatigue damage if they are preceded by even a few cycles of overloading, particularly those which cause local plastic buckling deformations at the fastener holes. This is because of the creation of plastic strains at some isolated points and/or the entire zone around the fastener holes during the initial few cycles of overloading. Therefore it may be necessary that the occurrence of even a few cycles of loading above the LPD load should be made rather unlikely by choosing a lower design load.

Considering the foregoing discussions, it may be appropriate to either reduce the current design load or to increase the LPD load of corrugated roofing. Obviously the building industry would prefer the latter approach and the use of cyclone washers can just do that. However, as the use of such washers is not so popular among the builders, one should investigate the possibility of increasing the LPD load by other means.

The LPD load is dependent on the geometry of the corrugated profile and the material properties. As the strength of the roofing material used at present is already high at the expense of loss of ductility, any attempt to increase the strength of the material further to achieve a greater LPD load may not be prudent. However, an attempt to determine the optimum geometry that would give the greatest LPD load is worthwhile, keeping in mind that major changes cannot be made to alter the overall appearance of the corrugated profile. To the author's knowledge, no analytical program is available that can be used to determine the LPD load and thus this investigation may have to be based on experiments alone. However, a lower bound load based on the first yield

point in the vicinity of the central support fastener holes can be determined for each geometry of the profile chosen using a finite element analysis. This task of achieving the greatest LPD load for the corrugated roofing profile may appear to be tedious, but if completed would give some useful results to the building industry.

The other parameter that could affect the LPD load is the ductility of the roofing material. During static tests, yielding occurred first at a point in the vicinity of the fastener holes, but spread rapidly to other points in the vicinity due to the absence of sufficient ductility of material currently used (see Section 3.3). Once sufficient yielding has developed around the fastener hole, the local plastic buckling occurred. Hence by using a ductile material for the same geometry, one could increase the LPD load as yielding would not spread rapidly in this instance. But it is not known by how much it will be increased. It is thought that the improvement in the LPD load through the use of a ductile roofing material may not produce similar improvement in the fatigue strength. This is because the ductility of the material can only delay the local plastic buckling, but yielding would have already commenced in the vicinity of the fastener holes. To confirm this, a static test and a fatigue test were conducted on corrugated roofing of almost identical geometry, but that was rolled from a low strength steel and greater ductility. The static test did show the presence of a greater LPD load, but the fatigue performance did not improve to the same degree as shown by the fatigue test. Hence it appears that greater ductility alone may not improve the fatigue performance significantly as anticipated.

The LPD load may also depend on the shape and size of the fastener head and the neoprene washer underneath, and on the size of fastener hole. During the initial stages of this investigation, it was believed that by increasing the size of the fastener head it could be possible to prevent premature cracking. But according to the manufacturers of roofing fasteners, the size of fastener head cannot be increased without increasing the shank diameter, using the current fastener production techniques. Tests were conducted on 650 mm test span roofing fastened at alternate crests with a circular washer that was about twice the diameter of the fastener head. The LPD load was still 650 N/f and the cyclic loading from zero to 650 N/f failed the specimen after only 820 cycles. There was only a slight increase in  $N_f$  due to the fact that now a bigger washer had to pull through the roofing. Therefore one could say that the change in geometrical parameters mentioned earlier in this paragraph cannot cause a significant improvement in the LPD load unless drastic changes are made, for example, the fastener head and neoprene washer have to be modified to be somewhat equivalent to cyclone washers.

In summary it appears that the fatigue performance of roofing fastened at alternate crests cannot be improved unless cyclone washers are used. Although the roofing at its current design load may satisfy the TR440 test requirements, the current design load is very close to the observed LPD load and as such there is very little safety margin to allow for uncertainties.

### 5.2.2 Alternate crest fastening with cyclone washers

Even for roofing fastened with cyclone washers, the fatigue behaviour was very much dependent on its LPD load. For roofing of 650 mm test span, representing a prototype span of 900 mm, the LPD load was 900 N/f. The fatigue performance deteriorated rapidly when the applied maximum cyclic load was greater than the LPD load. Therefore the LPD load is to be considered the ultimate load from a fatigue strength viewpoint even for roofing fastened with cyclone washers. Similar observations were made in the previous section for roofing fastened without cyclone washers.

The manufacturer of corrugated roofing uses a design load of 685 N/f for roofing fastened with cyclone washers (LBI, 1987). Unlike in the case of alternate crest fastening without cyclone washers, there appears to be a better safety margin when one compares the design load of 685 N/f with the observed LPD load of 900 N/f. This is also confirmed by the fatigue test results. It can be seen from Figure 14 that roofing can withstand approximately 63,000 cycles of loading from zero to its current design load. However, it was noted during this investigation that cyclone washers became ineffective when roofing was overloaded by 35% above design load. This was attributed to the thinner washers (1 mm) currently used. If a few cycles of overloading by more than 35% above the design load occurs relatively early during a cyclone, the cyclone washers will become ineffective and could lead to severe roofing damage in the following cycles of lower loading. A thicker washer will eliminate such occurrences because a similar overload may not damage the washers so much and the LPD load also will be increased. However, it is to be noted that such an overloading by more than 35% above design load is rather unlikely to occur.

At present corrugated roofing can be fastened at alternate crests with or without cyclone washers, but the corresponding design loads of 685 and 550 N/f should be used in selecting the spans to resist the design uplift wind pressure. However, the roofing with these fastening systems designed as above will not have the same margin of safety. Ideally all the building components designed using building codes and regulations should have a safety index of the same order. But in this instance, the roofing fastened with cyclone washers would withstand about 63,000 cycles whereas the roofing fastened without cyclone washers would fail after only about 2,200 cycles at their respective design load levels. This is further highlighted by a fatigue damage calculation using Miner's law in Table 9. When alternate crests are fastened without cyclone washers the damage caused by a TR440 loading sequence is 0.196 whereas it is a mere 0.003 when cyclone washers are used. Although there may be some doubts about the accuracy with which Miner's law can predict the fatigue damage of roofing, it is valid to use the results comparatively. The damage values in Table 9 are therefore essentially used to compare the two fastening systems.

**Table 9. Fatigue Damage Caused by TR440 Loading Sequence**

Applied Cycles	Without Cyclone Washers			With Cyclone Washers		
	Load (N/f)	N <sub>f</sub>	Damage	Load (N/f)	N <sub>f</sub>	Damage
8000	344	185,110	0.043	428	1.5x10 <sup>7</sup>	0.0
2000	413	32,780	0.061	514	1.8x10 <sup>6</sup>	0.0
200	550	2,175	0.092	685	62,650	0.003
			<u>0.196</u>			<u>0.003</u>

These observations highlight the difference in risk of failure by low cycle fatigue between these two accepted methods of fastening the same roofing. There is not enough information presently available to ascertain whether the inherent safety (from the engineering viewpoint) of the roofing without cyclone washers should be questioned. It is anticipated that the random load tests, currently under way, will provide that information.

### **5.3 Current Situation Regarding Safety of Roofing subjected to Cyclonic Wind Loading**

This investigation was mainly aimed at studying the fundamental fatigue behaviour of corrugated roofing assemblies using constant amplitude fatigue tests. No test was conducted using a realistic random load sequence or any programmed loading sequence like the one recommended by TR440 to represent cyclonic wind forces. Hence this investigation does not provide a definite answer regarding the safety of corrugated roofing assemblies subjected to cyclonic winds. Since 1978 all roofing installations are based on TR440 fatigue tests (except in N.T. where DABM test is used), and therefore should withstand cyclonic wind forces. Among these two fatigue testing methods, the latter is many times a severe test than the former. However, it is not known whether the TR440 loading sequence does in fact represent cyclonic wind forces on the conservative side. The results of the ongoing investigation to review the TR440 loading sequence combined with those from the present investigation should provide a definite answer to the safety of corrugated roofing assemblies in the near future.

A situation that causes concern regarding the use of alternate crest fastening without cyclone washers is when metal roof claddings act as a diaphragm. It is now believed that diaphragm action of metal roof claddings is present in low rise buildings whether the designer acknowledges it or not. Recent tests on full scale houses by the Cyclone Testing Station have shown that in addition to ceiling cladding the roof cladding also acted as a diaphragm in transferring the racking forces to the bracing walls (Reardon, 1986). Thus during a cyclone, light gauge metal roof claddings may be subjected not only to cyclonic uplift forces, but also to in-plane shear forces

unless separate roof bracings are provided. Under this combined loading, roofing fastened at alternate crests without cyclone washers is expected to perform inferior to that fastened with other systems considered in this report. The use of cyclone washers will provide greater safety against the combined action of cyclic uplift and in-plane shear forces. The Cyclone Testing Station is currently investigating the effects of combined uplift and in-plane shear forces on the fatigue behaviour of roofing fastened at alternate crests.

All the foregoing discussions indicate that alternate crest fastening with cyclone washers is the most suitable fastening system for corrugated roof claddings. If other fastening systems are to be used they should be designed to have the same margin of safety as in the cyclone washer fastening system.

Various measures can be taken in order to popularise the use of cyclone washers among the builders such that they are used voluntarily. It may be possible to develop a special attachment to the electric drill such that it holds the metal washers in position while the fasteners are being driven in. Initial attempts have been made already to achieve this, but progress will depend entirely on the response of the building industry.

#### **5.4 Other Roofing Profiles**

In this investigation no fatigue test was conducted on other roofing profiles. However, it is possible to predict fatigue behaviour of other roofing profiles based on results obtained for corrugated roofing and some limited static test results on an other profile (Mahendran, 1988b). In general, all the light gauge metal roofing profiles currently available in Australia fall into two main groups. The first group has crests and valleys of similar shape, with the crests spaced approximately 75 mm apart, as in corrugated and spandek profiles. The roofing is fastened either at alternate crests or at every third or fourth crest (LBI, 1987). The results obtained for corrugated roofing can be used to predict the behaviour of other profiles falling in this group. All roofing profiles in this group will have an LPD type behaviour.

The second group has ribs separated by wide pans, as in Trimdek profile (LBI, 1987) and other decking profiles. They are fastened at every crest. The static test conducted on a ribbed decking profile showed the presence of large cross-sectional distortion as the wide pans deflected upwards quite significantly (Mahendran, 1988b). However, there was no local plastic buckling deformation at the crests, instead localized yielding associated with smaller dimple formation occurred under the screw heads at approximately 50% of its ultimate static failure load. Yielding around the screw holes in this case was more localized than in the case of yielding associated with local plastic buckling of corrugated roofing. Because of this large stress concentration at the fastener holes, premature fatigue cracking may occur for the roofing profiles in this group despite the absence of LPD stages. The results from previous fatigue tests on such profiles conducted

by the Cyclone Testing Station confirm this. Even for this group of roofing profiles load per fastener will be the governing parameter for fatigue. An investigation into the effect of cyclic loading on one of the second group roofing profiles (Trimdek) is currently being conducted jointly by the Cyclone Testing Station and Curtin University of Technology. The investigation is in its early stages, but when completed, should verify the predictions made in this report.

In summary large cross-sectional distortion and stress concentrations at the fastener holes are present in both groups of profiles. Stress levels reach yielding value prematurely in both cases. The first group of profiles undergoes local plastic buckling deformation whereas the second group has a very much localized yielding. Both groups are therefore susceptible to fatigue cracking unless some form of cyclone washers are provided on the crests. In the second group the use of cyclone washers is potentially more effective than in the first group and may even completely eliminate fatigue cracking because there will be no localized yielding even at higher load levels closer to ultimate static failure load. It is to be noted that the use of cyclone washers for roofing in the first group does not eliminate fatigue cracking, but makes it much less likely to occur.

If attempts are made to develop alternative roof cladding-fastener assemblies for cyclone prone areas, they should aim towards such roofing profiles and fastening systems that will minimise any stress concentrations at the fastener holes. It will be beneficial if such an assembly can also create a pre-tension in the fasteners and the roof cladding material has sufficient ductility.

## 5.5 Future Work

None of the investigation on fatigue behaviour of corrugated roofing assemblies to date included a metallurgical study of the cracked regions. In this investigation various crack types were observed depending on the fastening system used and the peak load levels of the load cycle. A metallurgical study of these cracked regions could produce useful results which could explain many observations that could not have been explained otherwise. Various microscopic mechanisms responsible for initiation of such fatigue cracks observed in this investigation including the role of microstructure can be studied. Additional constant amplitude fatigue tests may have to be conducted in order to follow the changes in microstructure from initiation till failure. Initial steps have been already taken to carry out such an investigation in the future.

Fatigue life of corrugated roofing assemblies is affected significantly by crack propagation stages. Since no initial crack or flaw was observed prior to testing, fatigue life was affected by a crack initiation stage too. Hence an investigation on fatigue crack initiation and propagation using a fracture mechanics approach should provide comprehensive information on fatigue behaviour of corrugated roofing. Depending on the type of fracture (elastic or plastic), elastic-plastic fracture mechanics principles or linear elastic fracture mechanics principles may be used.

Despite the fact that the present problem of fatigue induced fracture at the localized area around the fastener hole is quite complicated such an investigation should be attempted in the future.

The reason for premature fatigue cracking in the corrugated roof claddings is well established as that due to the presence of large stresses and LPD behaviour at the fastener holes. However, there could be another reason if the steel has cyclic softening properties. Since cyclic softening is characteristic of cold worked metals, it is likely to be the case here. If the steel softens drastically under cyclic loading, plastic strains may appear at 50% of the monotonic yield stress, and thus cause premature fatigue cracking. Therefore an investigation on cyclic stress-strain behaviour of the steel used in roll-forming corrugated roofing is desirable to determine whether this steel has any cyclic softening properties.

## **5.6 Other Comments**

Once the adequacy of current standard fatigue testing methods is established or alternative methods adopted, roofing assemblies can be designed to have adequate fatigue strength using the results obtained in this investigation. However, it is in the best interests of the community to advise them to inspect the roof claddings of their houses in a manner similar to aircraft structures. This is because the fatigue damage accumulates in metal claddings, unlike in glazing which has a tendency to heal after every storm (Dalglish, 1979). Therefore roof claddings should be inspected for any cracks in roofing, damaged washers or corroded fasteners and roofing at the beginning of a cyclone season and also after a severe storm or cyclone, and if necessary repairs made or the roofing be stripped and replaced. This approach is based on the well-known fail-safe method applied to components loaded in fatigue. Such a concerted action from every member of the community is essential in addition to proper design of metal roof claddings, if fatigue failures are to be eliminated completely.

## **6. CONCLUSIONS AND RECOMMENDATIONS**

The following conclusions and recommendations have been made based on this fatigue investigation on corrugated roofing.

- (1) The fatigue behaviour of corrugated roofing assemblies subjected to cyclic uplift wind loading was very much dependent on the way roofing was fastened.
- (2) Fatigue test results of corrugated roofing with different spans and fastening systems correlated well with the corresponding static results obtained from an earlier investigation.

- (3) Results from this investigation, based on constant amplitude load testing of roofing assemblies, were adequate to gain a basic understanding of the fatigue behaviour of corrugated roofing. However, another investigation is already under way to review current fatigue testing methods and to study the fatigue performance of the same roofing assemblies under programmed loading and randomized block programmed loading sequences which simulate the cyclonic wind loading more closely.
- (4) With regard to the fatigue strength of roofing, alternate crest fastening with cyclone washers, alternate valley fastening and every crest fastening were found to be superior to the most commonly used alternate crest fastening system without cyclone washers. However, alternate valley fastening and every crest fastening cannot be recommended due to their potential shortcomings of water leakage and timber splitting, respectively.
- (5) When roofing fastened at alternate crests without cyclone washers was subjected to cyclic loading from zero minimum load,
  - (a) All the fatigue curves had different segments because of the local plastic buckling (LPD) behaviour.
  - (b) Large stress concentrations in a small region around the central support fastener holes caused low cycle fatigue cracking for all the spans of roofing. When the maximum cyclic load approached or exceeded the LPD load, the fatigue performance deteriorated rapidly due to the fact that the same region yielded at the LPD load.
  - (c) The presence of reserve static strength beyond the LPD load is of no importance from a fatigue point of view and the LPD load should be considered the ultimate fatigue load.
  - (d) Fatigue test results confirm the susceptibility to low cycle fatigue cracking of roofing fastened at alternate crests. Cracks always initiated at the bottom surface of roofing and propagated until failure when fasteners pulled through the roofing.
  - (e) Four different crack types were observed. The type of crack formed was mainly related to the maximum cyclic load.
  - (f) Microscopic examination of fastener holes prior to loading showed no crack-like defects due to drilling. Cracks were therefore initiated by large stress concentrations.
  - (g) Cycling at lower load levels also caused severe fatigue damage when it was preceded by only a few cycles of overloading, particularly those above the LPD load.
  - (h) Initial tightening of fasteners improved the fatigue performance significantly as the actual range of cyclic loading was reduced.



- (6) When roofing fastened at alternate crests without cyclone washers was subjected to cyclic loading from nonzero minimum load,
  - (a) Results revealed that not only the maximum cyclic load was a critical fatigue parameter, but also the range of loading.
  - (b) There was an anomalous observation due to the presence of LPD load. When mean level of loading was increased for a fixed value of range, the number of cycles to failure  $N_f$  first decreased as expected, but increased once the range of cycling extended above the LPD load. However, there was no such anomalous observation when range of loading was increased for a fixed mean level of loading.
  - (c) Two additional crack types were observed in this case when the maximum cyclic load was increased above the LPD load.
- (7) A comprehensive data base on the fatigue failure characteristics of corrugated roof claddings fastened at alternate crests without cyclone washers is now available in the form of a matrix and is being used along with results from wind tunnel investigations to review the current standard fatigue testing methods.
- (8) When alternate crests were fastened with cyclone washers,
  - (a) Fatigue performance was significantly improved because the region around the fastener hole was free of large stress concentrations. The LPD stage was still present, but at a greater load level and as such there were different segments in the fatigue curve.
  - (b) Fatigue cracking, propagation and eventual pull through of the entire washer assembly still occurred. However, this occurred after a very large number of cycles of loading when the maximum cyclic load was less than the LPD load. In this instance cracking first appeared under the washer edges in the longitudinal direction due to the presence of large stresses at this location.
  - (c) Once the maximum cyclic load was greater than the LPD load, the fatigue performance rapidly deteriorated as if there were no cyclone washers, not only because the load cycling had to go through LPD stages, but also because the thin washers became ineffective at the end of first cycle.
  - (d) An overloading by 35% above the current design load level caused a severe reduction of roofing's life span as it made the cyclone washers ineffective. The use of thicker washers will safeguard roofing against such overloading.

- (e) Three types of extensive cracking patterns were observed depending on the maximum cyclic load level.
- (9) For roofing fastened at alternate crests with and without cyclone washers, empirical mathematical equations were derived to predict the  $N_f$  in the case of zero minimum load. A general equation was derived to include all cases of loading for roofing fastened at alternate crests without cyclone washers.
  - (10) The two recommended fastening systems of alternate crest fastening with and without cyclone washers do not provide the same degree of safety against fatigue failure. It may be necessary to reduce the current design load of roofing fastened without cyclone washers. Alternatively, attempts could be made to increase the LPD load by optimising the geometry of corrugated profile.
  - (11) When every crest was fastened, fatigue performance was significantly improved and the fatigue curves were simple continuous curves as no LPD behaviour was observed in this case. However, fatigue cracking still occurred at the crests where larger stresses were found, but not prematurely at lower load levels.
  - (12) When alternate valleys were fastened,
    - (a) Fatigue performance was significantly improved due to the absence of LPD behaviour and any dimpling of crests. However, fatigue curves were not smooth continuous curves due to the large cross-sectional distortion and the resulting stiffening at higher load levels.
    - (b) Crack types were quite different to those observed in other cases.
  - (13) When alternate crests were fastened without cyclone washers, load per fastener was the most critical parameter controlling the fatigue behaviour up to the LPD load. However, for all other fastening systems, both load per fastener and bending moment at the central support were found to be critical fatigue parameters.
  - (14) In all cases of roofing with different fastening systems and spans at various load levels, appearance of a crack did not mean an imminent failure. Crack propagation stages contributed significantly to the fatigue life of roofing assembly.
  - (15) Based on a limited number of tests, the effect of loading frequency on fatigue test results was found to be insignificant in the range of frequency that can be used in practice. A suggestion to revise the relevant clause 2.4 (f) of TR440 regarding loading frequency has been made.

- (16) It is essential that current fatigue test loading sequences simulate the cyclonic wind loading more closely on the conservative side. Otherwise the light gauge metal roofing assemblies which are found to be susceptible to fatigue damage may fail during cyclonic winds.
- (17) Although the results obtained in this investigation are applicable mainly to corrugated roofing assemblies, they can be used effectively to predict the fatigue behaviour of most other light gauge metal roofing assemblies, or to eliminate any weaker roofing systems, or to develop alternative systems.
- (18) Future investigations on corrugated roofing regarding the effects of combined uplift and in-plane shear forces on fatigue cracking, fatigue crack initiation and propagation using fracture mechanics approach, metallurgical aspects of fatigue behaviour and cyclic softening properties of the steel should provide useful and interesting results to supplement those obtained already in this investigation.

## 7. ACKNOWLEDGEMENTS

The author wishes to thank

- (1) Lysaght Building Industries for donating the corrugated roof sheeting to the Cyclone Testing Station's specifications,
- (2) W.A. Deutsher Pty. Ltd. for donating the fasteners,
- (3) the Station's Technical Director, Mr G.F. Reardon and Professor G.R. Walker of the Dept. of Civil and Systems Engineering, James Cook University for their support and guidance in this research project and
- (4) the Station's technical staff, Messrs. W. Morris and K. Abercombie for their technical assistance.

The author appreciates the valuable help of Mr. Reardon in the preparation of this report.

## 8. REFERENCES

- Atkins, A.G. and Mai, Y.W. (1985) Elastic and Plastic Fracture, Ellis Horwood, England.
- Beck, V.R. (1977) Random Wind Loading on Metal Roof Cladding, Paper presented to the Workshop on Guidelines for Cyclone Product Testing and Evaluation, Experimental Building Station, Sydney, July.
- Beck, V.R. (1978) Wind Loading Failures of Corrugated Roof Cladding, M.Eng.Sc. Thesis, Dept. of Civil Engineering, University of Melbourne.

Beck, V.R. and Morgan, J.W. (1975) Appraisal of Metal Roofing under Repeated Wind Loading - Cyclone Tracy Darwin 1974, Australian Dept. of Housing and Construction, Housing Research Branch, Tech. Rept. No.1, Feb.

Beck, V.R. and Stevens, L.K. (1979) Wind Loading Failures of Corrugated Roof Cladding, Civil Eng. Transactions, I.E.Aust., Vol. CE21, No.1, pp. 45-56.

Dalglish, W.A. (1979) Assessment of Wind Loads for Glazing Design, Paper presented at the IAHR/IUTAM Symposium on Practical Experiences with Flow-induced Vibrations, Karlsruhe, Germany, Sept.

Darwin Reconstruction Commission (DRC) (1976), DABM - Darwin Area Building Manual, Darwin.

D'Isa, F.A. (1968) Mechanics of Metals, Addison-Wesley, USA.

Eaton, K.J. and Mayne, J.R. (1974) The Measurement of Wind Pressures on Two-storey Houses at Aylesbury, Current Paper CP 70/74, Building Research Establishment, Dept. of Environment, U.K., July.

Ekvall, J.C. and Young, L. (1976) Converting Fatigue Loading Spectra for Flight-by-Flight Testing of Aircraft and Helicopter Components, J. of Testing and Evaluation, Vol.4, No.4.

Experimental Building Station (EBS) (1978) TR440 - Guidelines for the Testing and Evaluation of Products for Cyclone Prone Areas, Sydney.

Jancauskas, E.D.J., Walker, G.R. and Mahendran, M. (1989) Fatigue Characteristics of Wind Loads on Roof Cladding, Paper to be presented at the 2nd Asia-Pacific Symposium on Wind Engineering, Beijing, China, June.

Lysaght Building Industries (1987), LBI Reference Manual.

Mahendran, M. (1988a) Static Analysis of Corrugated Roofing under Simulated Wind Loading, Proc. of the 11th ACMSM Conference, Auckland, New Zealand, pp. 213-218.

Mahendran, M. (1988b) Static Behaviour of Corrugated Roofing under Simulated Wind Loading, Technical Report No.33, Cyclone Testing Station, James Cook University.

Mahendran, M. and Reardon, G.F. (1988) The Behaviour of Corrugated Roofing under Simulated Static and Cyclic Wind Loads, Paper presented to the Workshop on Review of TR440 - Guidelines for the Testing and Evaluation of Products for Cyclone Prone Areas, National Building Technology Centre, Sydney.

- Mann, J.Y. (1974) Objectives and Procedures in Fatigue Testing, Mech. and Chem. Eng. Transactions, I.E.Aust., Vol. MC10, pp. 4-9.
- Melbourne, W.H. (1977) Loading Cycles for Simulation of Wind Loading, Paper presented to the Workshop on Guidelines for Cyclone Product Testing and Evaluation, Experimental Building Station, Sydney, July.
- Morgan, J.W. and Beck, V.R. (1977) Failure of Sheet-metal Roofing under Repeated Wind Loading, Civil Eng. Transactions, I.E. Aust., Vol. CE19, No.1, pp.1-5.
- Neal, T.P. (1984) The Structural Performance of Nail-fixed Corrugated Steel Roof Cladding, Technical Report, Building Research Association of New Zealand, Wellington, New Zealand.
- Owen, D.R.J. and Fawkes, A.J. (1983) Engineering Fracture Mechanics : Numerical Methods and Applications, Pineridge Press Ltd., Swansea, U.K.
- Pook, L.P. (1978) An Approach to Practical Load Histories for Fatigue Testing Relevant to Off-shore Structures, J. Soc. Env. Engrs., 17-1.
- Reardon, G.F. (1980) Recommendations for the Testing of Roofs and Walls to Resist High Wind Forces, Technical Report No. 5, Cyclone Testing Station, James Cook University.
- Reardon, G.F. (1986) Simulated Cyclone Wind Loading of a Brick Veneer House, Technical Report No. 27, Cyclone Testing Station, James Cook University.
- Reardon, G.F., Walker, G.R., and Jancauskas, E.D. (1986) Effects of Cyclone Winifred on Buildings, Technical Report No. 28, Cyclone Testing Station, James Cook University.
- Rolfe, S.T. and Barsom, J.M. (1977) Fracture and Fatigue Control in Structures - Applications of Fracture Mechanics, Prentice-Hall, Englewood Cliffs, New Jersey, USA.
- Slogrove, T. (1985) Investigations of Fatigue Failure of Steel Cladding under Wind Loads, B.Eng. Thesis, James Cook University.
- Standards Association of Australia (SAA) (1984) AS 1397 - Steel Sheet and Strip - Hot-dipped Zinc-coated or Aluminium/Zinc-coated.
- Standards Association of Australia (SAA) (1977) AS 1445 - 76 mm pitch Corrugated hot-dipped Zinc-coated or Aluminium/Zinc-coated Steel Sheet.
- Walker, A.C. and Kwok, M.K. (1988) Fatigue Cracking in Damaged Cylinders Subjected to Cyclic Compressive Loading, Proc. of the N.W. Murray Symposium - Thin-walled Structures : Developments in Theory and Practice, Monash University, Melbourne, November.

Walker, G.R. (1975) Report on Cyclone Tracy - Effect on Buildings - Dec. 1974, Vol.1, Australian Dept. of Housing and Construction, Melbourne.

Walker, G.R. (1980) A Review of the Impact of Cyclone Tracy on Australian Building Regulations and Practice, Civil Eng. Transactions, I.E.Aust., Vol. CE22, No.2, pp.100-107.

Walker, G.R. (1984) Wind Induced Fatigue in Static Structures, Chapter 3 in Wind Engineering Handbook of Building Research Establishment, U.K.

Walker, G.R. and Reardon, G.F. (1986) A Discussion of Criteria for the Structural Design of Buildings to Resist Tropical Cyclones, Technical Report No. 29, Cyclone Testing Station, James Cook University, December.